Aus dem Institut für Humangenetik
der Ludwig-Maximilians-Universität München
Direktorin: Prof. Dr. med. Ortrud Steinlein

Nuclear orientation patterns for mouse chromosome 11 in normal B lymphocytes and during plasmacytoma development

Dissertation
zum Erwerb des Doktorgrades der Medizin
an der Medizinischen Fakultät der
Ludwig-Maximilians-Universität zu München

vorgelegt von
Ann-Kristin Victoria Schmälter
aus Bonn
2017

Mit Genehmigung der Medizinischen Fakultät der Universität München

Berichterstatter:	Prof. Dr. Ortrud Steinlein
Mitberichterstatter:	Prof. Dr. Axel Imhof
	Jun. Prof. Dr. Dr. Lesca M. Holdt
Mitbetreuung durch den promovierten Mitarbeiter:	PD Dr. Stefan Müller
Dekan:	Prof. Dr. med. dent. Reinhard Hickel
Tag der mündlichen Prüfung:	12.01.2017

Table of contents

Abbreviations

2D	Two-dimensional
3D	Three-dimensional
CT	Chromosome territory
DEAC	7-diethylaminocoumarin-3-carboxliyc acid
FACS	Fluorescence-activated cell sorting
FISH	Fluorescence *in situ* hybridization
FITC	Fluorescein isothiocyanate
mBANDing	multicolor banding
PCT	Plasmacytoma
Pre B cells	Mouse Pre B lymphocytes of BALB/c origin
T38Hwt lymphocytes	primary B lymphocytes of congenic [T38HxBALB/c]N wild-type mice
T38HT(X;11) lymphocytes	B lymphocytes of [T38HxBALB/c]N mice with a reciprocal translocation between chromosome X and 11

List of publications

Schmälter AK, Righolt CH, Kuzyk A, Mai S. Changes in nuclear orientation patterns of mouse chromosome 11 during mouse plasmacytoma development. **Transl Oncol.** 2015 Oct;8(5):417-23. doi: 10.1016/j.tranon.2015.09.001.

Righolt CH, **Schmälter AK**, Kuzyk A, Young IT, van Vliet LJ, Mai S. Measuring murine chromosome orientation in interphase nuclei. **Cytometry A**. 2015 Aug;87(8):733-40. doi: 10.1002/cyto.a.22674.

Schmälter AK, Kuzyk A, Righolt CH, Neusser M, Steinlein OK, Müller S, Mai S. Distinct nuclear orientation patterns for mouse chromosome 11 in normal B lymphocytes. **BMC Cell Biology**. 2014 Jun 12;15:22. doi: 10.1186/1471-2121-15-22.

Wiener F, **Schmälter AK**, Mowat MRA, Mai S. Duplication of sub-cytoband 11E2 of chromosome 11 is always associated with accelerated tumor development in *v-abl/myc* induced mouse plasmacytomas. **Genes & Cancer.** 2010 Aug;1(8):847-58. doi: 10.1177/1947601910382897.

1 Introduction

This cumulative dissertation includes the two publications “Distinct nuclear orientation patterns for mouse chromosome 11 in normal B lymphocytes” published in BMC Cell Biology in June 2014 and “Changes in nuclear orientation patterns of mouse chromosome 11 during mouse plasmacytoma development” published in Translational Oncology in October 2015.

1.1 Background

Epigenetics is a term describing the process of modifications of chromosomes. These modifications occur without changing the genotype but influence gene activity and gene expression. Adrian Peter Bird defines epigenetics as “the structural adaption of chromosomal regions so as to register, signal or perpetuate altered activity states”(Bird 2007). Russo describes epigenetics as "the study of mitotically and/or meiotically heritable changes in gene function that cannot be explained by changes in DNA sequence" (Russo, Martienssen, and Riggs 1996). Chromosomes consist of chromatin which in turn is composed of DNA, RNA and proteins, primarily histones. Epigenetic modifications of chromatin include methods like DNA methylation or histone acetylation (Kouzarides 2007). The exact structural organization of chromatin has not been identified up to date.

Different aspects of nuclear architecture may also have an influence on epigenetic changes. Chromosomes are organized in chromosome territories (CT). These are specific regions within the three-dimensional (3D) nucleus, which are evolutionary conserved (Cremer and Cremer 2010). The arrangement of CTs is dependent on factors like chromosome size, gene density or for example gene activity. Transcriptionally active genes can be found outside of CTs whereas inactive genes are located inside (Morey, Kress, and Bickmore 2009). 3D FISH studies to clarify the structure and organization of CTs are of enormous relevance for a better understanding of nuclear architecture.

1.2 Orientation

Analyzing orientation patterns of chromosomes in the 3D nucleus is a new approach in studying nuclear architecture. The regions at the end of eukaryotic chromosomes are

called telomeres, which consist of repetitive nucleotide sequences to protect the chromosome from degradation (Chan and Blackburn 2004). The centromere is the region where the two chromatids of a chromosome are connected before chromosome division during mitosis. The centromere can be located at different positions on the chromosome, e.g. metacentric, acrocentric or telocentric. Mouse chromosomes have only telocentric centromeres at the terminal end of chromosomes (Kalitsis, Griffiths, and Choo 2006). In our publications this end is referred to as “centromeric end”.

In both studies we assessed the orientation of chromosome 11 in the 3D nucleus of murine cells. Telomeric and centromeric ends of chromosomes can indicate the orientation of the whole chromosome, which may for example either point towards the nuclear center or towards the periphery. In addition, chromosomes can also be located in parallel to the nuclear border with the end neither pointing towards the nuclear center nor the periphery. Determining the orientation of homologous chromosomes results in various orientation patterns: Both homologs can point with their telomeric ends towards the nuclear center (1), both can point with their centromeric ends towards the center (2), both can be located in parallel to the nuclear border (3), one can be in parallel whereas the other points with its centromeric end (4) or telomeric end (5) towards the center. Alternatively, one homolog can be oriented with its telomeric end towards the center whereas the other points with its centromeric end towards the center (6). Analysis was performed by visual inspection and by the use of automatic programs. For the visual inspection, a parameter assessing the parallel orientation of chromosomes was introduced during evaluation of nuclear orientation patterns. Automated analyses classified the parallel orientation into a direction (i.e. one end towards the center and one towards the periphery since a perfect parallel orientation did not exist).

1.3 Chromosome 11

In the center of interest was chromosome 11 because it is frequently altered in mouse plasmacytoma (PCT) which is a B cell lineage tumor. Wiener et al discovered 2010 that subcytoband 11E2 of mouse chromosome 11 is regularly duplicated in mouse fast-onset PCTs. Moreover, they indicated that it accelerates PCT development. In these PCTs a high frequency of subcytoband 11E2 trisomy was found, associated with the overexpression of genes within 11E2. The corresponding syntenic regions in human are 17q25 and 10q32 in rat and they are regularly changed in many tumors (Kuzyk et al. 2015; Turhan et al. 2006; Koelsch, Rajewsky, and Kindler-Rohrborn 2005; Langan

et al. 2004). Subcytoband 11E2 may therefore play an important role in the tumorigenic process.

1.4 Aim

The focus of both publications was the study of mouse chromosome 11 orientation patterns in the 3D interphase nucleus of tumor and control cells. Orientation patterns have never been assessed before, so we analyzed normal lymphocytes at first and lymphocytes deriving from PCT subsequently. We examined whether chromosome 11 was oriented with its telomeric or centromeric end towards the nuclear center, respectively periphery or whether it showed a parallel position to the nuclear border. Distinct orientation patterns in nuclei of normal lymphocytes and of PCT cells were determined.

Multicolor banding (mBANDing) was used in order to determine the orientation in four different cell types. The orientation patterns were compared to each other and changes during tumor development were observed.

2 Material and Methods

2.1 Cell types

We examined four different cell types: Diploid mouse Pre B lymphocytes of BALB/c origin (Pre B cells), primary B lymphocytes of congenic [T38HxBALB/c]N wild-type mice (T38Hwt lymphocytes), B lymphocytes of [T38HxBALB/c]N mice with a reciprocal translocation between chromosome X and 11 (T38HT(X;11) lymphocytes) and fast-onset plasmacytoma (PCT) cells (Wiener et al. 2010). T38HT(X;11) lymphocytes exhibited a long chromosome (T(11;X)) and a short chromosome (T(X;11)). Fast-onset PCT cells are induced in the unique [T38HxBALB/c]N rcpT(X;11) mouse model by pristine and v-abl/myc. The mean latency of fast-onset PCTs is only 45 days.

Pre B cells were grown in cell culture, lymphocytes were harvested from the spleens of 6 to 8 week old T38Hwt and T38HT(X;11) mice and PCT cells were isolated out of the ascites of fast-onset PCT mice. To gain valid results we analyzed approximately 300 nuclei per cell type and about a hundred nuclei were used from each slide. Since studies were done in triplicate, we needed three mice per cell type.

2.2 Methods

To control copy number and structural stability of chromosome 11 and to verify the labeling of the mBAND paint, metaphase spreads of Pre B and T38Hwt lymphocytes were prepared and two-dimensional (2D) cell fixation was performed. Three slides of each cell type underwent hybridization with the chromosome 11 mBAND probe, which were conducted in three different experiments. 20 metaphases per slide were imaged using an Axioplan 2 microscope (Carl Zeiss Ltd., Toronto, ON, Canada) and the ISIS-FISH imaging system 5.0 SR 3 (Metasystems Group Inc. Boston, MA, USA).

3D fixation to nuclei of Pre B cells and of lymphocytes of T38Hwt, T38HT(X;11) and PCT mice was conducted after harvesting them from spleens, respectively ascites. 3D nuclei fixation was performed according to a protocol described by Solovei et al. 2002 (Solovei et al. 2002).

The method we used on all nuclei of all four cell types is mBANDing. Normally mBANDing is used to detect intrachromosomal rearrangements (Chudoba et al. 1999) but it can also be applied for studying nuclear architecture. Before fluorescence in situ

hybridization (FISH) the nuclei underwent 3D cell fixation. The chromosome 11 mBANDing paint consists of four different fluorochromes labeling four different overlapping segments of chromosome 11. The telomere is labeled with FITC (green), the pericentromeric region with Texas Red (magenta) and the segments in between in GOLD (red) and DEAC (cyan blue). In total 12 individual mBAND experiments were carried out. Using an AxioImager Z2 microscope, corresponding filters to the four fluorochromes and an AxioCam MRm (Carl Zeiss Inc. Canada) over 300 nuclei per cell type were captured, approximately 100 per slide. In order to reconstruct a 3D image, z-stacks of 80 slices with 200nm axial distance and 102nm lateral pixel size were acquired. After acquisition the images were deconvolved with a constrained iterative algorithm (Schaefer, Schuster, and Herz 2001) using the Axiovision Release 4.8 Software (Carl Zeiss Inc. Canada).

2.3 Analysis

For analyzing orientation patterns, we used three different methods. Firstly, we examined all nuclei by visual inspection. We determined whether the telomere pseudo-colored in green or the centromere pseudo-colored in red was pointing towards the nuclear periphery, respectively the nuclear center. When no end was oriented towards the center or periphery, these chromosomes were designated as parallel. The combination of different chromosome 11 orientations resulted in different orientation patterns. Polyploid nuclei with more than four copies of chromosome 11 were difficult to analyze visually. Therefore, only the orientation of chromosome 11 in nuclei with up to four copies was determined. The position of the small translocation chromosome T(X;11) whether it is located in a central, intermediate or peripheral nuclear position was also examined visually.

Secondly, for the first publication (“Distinct nuclear orientation patterns for mouse chromosome 11 in normal B lymphocytes”) 45 nuclei of Pre B cells and of T38Hwt lymphocytes were additionally analyzed with a semi-automatic quantitative program using the software eADS (Kupper et al. 2007). The program measured the distance in nanometer between the geometric centers of each chromosomal segment and the nuclear border. Afterwards the adequate orientation to each chromosome had to be assigned. Further, the conformation of chromosome 11 was assessed whether it showed a straight or angulated formation. The main disadvantage of the analysis by the semi-automatic program was that all chromosomes 11, each band and nucleus had to un-

dergo manual segmentation and therefore all pixels at different levels of grey had to be distinguished visually.

Thirdly, for the second publication (“Changes in Nuclear Orientation Patterns of Chromosome 11 during Mouse Plasmacytoma Development”) nuclei of PCT and T38H(TX;11) lymphocytes were additionally analyzed with a fully automated program. This program measures chromosome orientation in the 3D nucleus (Righolt et al. 2015) and it provides exact results. We therefore did not determine a parallel orientation any longer. Unfortunately, the program could only be implemented for diploid cells. In the second paper though we assessed PCT cells showing two and more copies of chromosomes 11. For statistical comparison of the orientation patterns the method of analysis had to be the same. Consequently, we used the results by visual inspection in both publications.

3 Results and Discussion

We analyzed orientation patterns of chromosome 11 in nuclei of a diploid mouse Pre B lymphocyte line of BALB/c origin, in B lymphocytes of congenic [T38HxBALB/c]N wild-type mice and [T38HxBALB/c]N rcpT(X;11) mice and of PCTs. We performed mBANDing to 3D preserved nuclei and examined more than 300 nuclei of each cell type. The mouse chromosome 11 mBAND probe labels four overlapping segments with four fluorescing colors. The telomeric end is labeled with FITC Green, the centromeric end with Texas Red and the regions in between with Gold and DEAC. The mBANDed nuclei were imaged using Axiovision 4.8 Software (Carl Zeiss Inc. Canada) and were deconvolved with a constrained iterative algorithm. By visual inspection we analyzed the orientation of chromosome 11 of the respective cell types and subsequently determined orientation patterns.

3.1 Chromosome 11 orientation patterns

We observed three different orientations; (1) chromosome 11 points with its telomeric end to the nuclear periphery and with its centromeric end to the nuclear center, (2) it points with its centromeric end to the nuclear periphery and with its telomeric end to the center, (3) chromosome 11 was designated as parallel to the nuclear surface when the end was pointing neither towards the nuclear center nor the periphery. Combining the observed orientations of all chromosomes in one nucleus, we determined an orientation pattern.

In the first study we observed three main patterns of chromosome 11 orientation in 3D interphase nuclei from Pre B and T38Hwt lymphocytes: The most frequent orientation pattern observed in both cell types was with both copies of chromosome 11 located in parallel to the nuclear border (37.3% and 31.9%, respectively). There was no significant difference in the occurrence of this orientation pattern between both lymphocyte types (p=0.20). The second most common orientation observed was with one homolog of chromosome 11 oriented with its telomeric end towards the nuclear center, while the other chromosome 11 homolog was found in parallel to the nuclear border (20.5% and 26.1% in Pre B and T38Hwt mouse lymphocytes, respectively). There was no significant difference in the frequency of this orientation pattern seen between both types of lymphocytes (p=0.13). One chromosome 11 pointing with its centromeric end to the center and the other located in parallel to the nuclear border was the third most fre-

quently observed orientation. The occurrence of this orientation pattern did not differ significantly in both types of lymphocytes (p=0.05) with a frequency of 16.3% in Pre B and of 10.4% in T38Hwt lymphocyte nuclei. There was a significant difference between the percentages of cells with each of the three major orientation patterns within each cell type ($p < 0.001$). There was no significant difference in the occurrence of the orientation patterns observed between both B cell types (p>0.05).

In the second study we examined chromosome 11 orientation patterns in nuclei of lymphocytes from PCT and T38HT(X;11) mice. The most frequently observed orientation pattern in T38HT(X;11) was with both chromosomes located in parallel to the nuclear border (35.0%). In all PCTs this orientation pattern was only observed in 10.7% (p<0.01). The orientation pattern with one homolog pointing with its centromeric end towards the nuclear periphery and the other homolog being in parallel was found most frequently in PCTs (13.4% of all PCTs) and in 23.7% of T38HT(X;11) (p=0.83). Both chromosomes pointing with their centromeric ends towards the periphery was observed in 18.7% of T38HT(X;11) and in 8.5% of all PCTs (p=0.0001). The third most common orientation pattern in PCTs was with one homolog located in parallel whereas the other homolog was pointing with its telomeric end to the periphery (8.5%). This orientation pattern was found in 13.6% of T38HT(X;11) nuclei (p<0.01). When comparing T38HT(X;11) nuclei to all PCT nuclei with respect to their orientation patterns a significant difference was noted (p<0.0001).

115 out of 224 (51.3%) PCT nuclei showed three or more copies of chromosome 11. Various orientation patterns were determined for all PCT nuclei with up to four chromosomes 11.

Moreover, we identified the position of the small translocation chromosome T(X;11) in all nuclei of T38HT(X;11) and PCT. T(X;11) carrying cytoband 11E2 was most frequently observed in the intermediate region of the nucleus. There is no significant difference between the two cell types regarding the position of T(X;11) (p=0.06).

3.2 Chromosome 11 3D conformation

The 3D conformation of 90 individual chromosomes 11 from Pre B and T38Hwt lymphocytes was evaluated by measuring angles between the geometric centers of the different mBAND probes in individual chromosomes using the software eADS (Kupper et al. 2007). We determined whether chromosome 11 is preferentially straight or angulated during interphase. 19% of Pre B and 15% of T38Hwt B cell chromosome 11 showed angles between 0 and 60° and were considered as angulated, whereas 47% of

Pre B and 43% of T38Hwt B cell chromosome 11 showed angles between 121° and 180°. These data indicate that mouse chromosome 11 shows a preferentially straight 3D conformation in both cell types.

3.3 FACS Analysis

To determine whether cell cycle distribution had an impact on the chromosome 11 orientation patterns, cell cycle profiles of Pre B and T38Hwt lymphocytes were measured by FACS analysis. As the Pre B lymphocytes were kept proliferating in culture, the cells were distributed throughout the different cell cycle phases with 45% in G0/G1, 44% in S and 21% in G2/M. In contrast, the majority of the T38Hwt cells were found in G0/G1 (94%) with only 5% in S and 2% in G2/M. The comparison of the distinct cell cycle profiles indicates that cell cycle stages have no influence on nuclear orientation.

3.4 Discussion

There are several reasons why studying orientation patterns is relevant for a better understanding of nuclear architecture and its impact on epigenetics. Firstly, chromosomes occupy specific evolutionary conserved CTs (Cremer and Cremer 2010), they are located in nonrandom positions in the 3D nucleus. The location of chromosome territories in the 3D nucleus is dependent e.g. on the activity, respectively inactivity of genes (Solovei et al. 2009; Dyer, Canfield, and Gartler 1989), gene-density (Kupper et al. 2007) or guanine-cytosine content (Hepperger et al. 2008). The question whether chromosomes show a distinct orientation within the CT was never asked before. Secondly, various studies show that distinct characteristics of the nuclear organization have an influence on e.g. transcription rate, differentiation or cell cycle (Mehta et al. 2010; Marella et al. 2009; Morey, Kress, and Bickmore 2009). Rotation of chromosomes is a possible mechanism of movement. Chromosomes may rotate to reach transcription factories. Chromatin changes its position (Lanctot et al. 2007) or loops out (Volpi et al. 2000) in order to be transcribed. In the examined fast-onset PCT the length of the telomere containing cytoband 11E2 is significantly increased (Kuzyk and Mai 2012). Rotation could lead to a closer proximity between a transcription factory and the genes of 11E2 in PCT cells. Thirdly, orientation may serve as a protection mechanism. Heride et al. 2010 showed that chromosomes are closer to heterologs than homologs which may avoid homologous recombination and damaging of both homologous copies (Heride et al. 2010). We observed in approximately 45% of the studied cells that the orientation of the chromosome 11 homologs was different. They may rotate or the ori-

entation may be conserved in its location to protect themselves from genotoxic stress. On the contrary rotation could lead to closer proximity of telomeres and the formation of telomeric aggregates resulting in telomere dysfunction and genomic instability (Mai and Garini 2006, 2005). However, the influence of orientation patterns on epigenetic modifications needs to be evaluated in further studies.

4 Summary

4.1 English version

Analyzing orientation patterns of chromosomes in the 3D nucleus using Fluorescence *in situ* hybridization (FISH) is a new approach to study nuclear architecture. Previous studies demonstrate that chromosomes are located in nonrandom positions in the nucleus, they occupy specific chromosome territories (CTs) (Cremer and Cremer 2010). In this context it was shown that characteristics of the nuclear organization like distinct positioning of chromosomes within the CT or mechanisms of chromatin movement have an influence on e.g. transcription rate, differentiation or cell cycle (Mehta et al. 2010; Marella et al. 2009; Morey, Kress, and Bickmore 2009). A study of Wiener et al. (2010) concerning numerical chromosomal aberrations of chromosome 11 in mouse plasmacytoma (PCT), which showed that subcytoband 11E2 of chromosome 11 is duplicated in fast-onset mouse PCT, gave rise to the question whether the aspect of orientation is significant for PCT development. Plasmacytoma is a malignant tumor deriving from lymphocytes of the B cell lineage and chromosome 11 aberrations are considered one of the most frequent chromosomal aberrations in mouse PCTs.

There are several possibilities regarding the orientation of chromosomes in the 3D nucleus. Chromosomes can either point with their telomeric or their centromeric end towards the nuclear periphery, respectively towards the nuclear center. Just as well they can be located parallel to the nuclear border with no end pointing towards the periphery or center. This is the first study to evaluate the orientation of chromosomes in the 3D nucleus. According to the study of Wiener et al. (2010) we first examined the orientation of chromosome 11 in normal B lymphocytes and subsequently in PCT cells. The focus of both our studies was the orientation of mouse chromosome 11 in the 3D interphase nucleus of four different cell types: The first publication (“Distinct nuclear orientation patterns for mouse chromosome 11 in normal B lymphocytes”) presents the results of the analysis of diploid mouse Pre B lymphocytes of BALB/c origin and primary B lymphocytes of congenic [T38HxBALB/c]N wild-type mice. The results of the analysis of B lymphocytes of [T38HxBALB/c]N mice with a reciprocal translocation between chromosome X and 11 (T38HT(X;11) lymphocytes) exhibiting a long (T(11;X)) and a short (T(X;11)) chromosome and of fast-onset PCT cells (Wiener et al. 2010) were presented

in the second publication ((“Changes in Nuclear Orientation Patterns of Chromosome 11 during Mouse Plasmacytoma Development”).

For displaying chromosome 11 in the 3D interphase nucleus we used multicolor banding (mBANDing) (Benedek et al. 2004). The specific mouse chromosome 11 mBAND probe hybridizes with four overlapping segments of the whole chromosome 11 painting it in four fluorescent colors. The telomeric end is labeled in green (FITC), the centromeric end in magenta (Texas Red) and the segments in between in red (Gold) and cyan blue (DEAC). We imaged approximately 300 nuclei per cell type using an AxioImager Z2 microscope, corresponding filters for the four fluorochromes and the Axiovision 4.8 software (Carl Zeiss Inc. Canada). The orientation of all chromosome 11 homologs was determined by visual inspection.

In the first study the most frequent orientation patterns observed in nuclei of Pre B and T38Hwt lymphocytes were with both chromosomes 11 in parallel to the nuclear border. The second most frequently found pattern was with one homolog located in parallel while the other was pointing with its telomeric end towards the nuclear center and with its centromeric end towards the periphery. There was no significant difference between Pre B and T38Hwt lymphocytes regarding chromosome 11 orientation patterns ($p>0.05$). To support these results a semi-automatic quantitative analysis was conducted.

In the second study nuclei of T38HT(X;11) lymphocytes also showed most frequently the orientation pattern with both chromosomes 11 located in parallel to the nuclear border. In PCT cells two or more copies of chromosome 11 were found. The most frequently observed orientation pattern in diploid PCT cells was with one chromosome 11 in parallel whereas the other was pointing with its centromeric end towards the nuclear periphery, and with its telomeric end towards the center respectively. There is a significant difference between the two studied cell types regarding chromosome 11 orientation patterns ($p<0.0001$). An additional analysis of the diploid cells using a fully automated program to measure the orientation of chromosomes in the 3D nucleus was conducted (Righolt et al. 2015).

Furthermore, in the first study the conformation of chromosome 11 using the software eADS (Kupper et al. 2007) was examined. Chromosome 11 showed a preferentially straight not angulated configuration. In addition, a fluorescent activated cell sorting (FACS) analysis of Pre B and T38Hwt cells was carried out. Pre B lymphocytes were distributed throughout all cell cycle phases whereas T38Hwt lymphocytes were found

particularly in G0/G1 phase. This indicates that chromosome 11 orientation is with a high probability independent of cell cycle phases.

The position of the small translocation chromosome T(X;11) in the 3D nucleus was assessed additionally in the second study. T(X;11) contains subcytoband 11E2 und parts of E1. The telomeric probe of the mBAND paint labels it in green (FITC) only. We examined whether the small translocation chromosome T(X;11) is either located in a peripheral, central or intermediate position of the 3D nucleus. In both PCT and T38HT(X;11) lymphocytes it was found most frequently in the intermediate.

In both publications we showed that there are distinct orientation patterns observed in all studied cell types. However, determining whether changes in the orientation patterns have an impact on PCT development, will have to be in the focus of further studies.

4.2 German version

Die Analyse der Orientierung von Chromosomen im 3D-Zellkern mittels Fluoreszenz-in-situ-Hybridisierung (FISH) ist ein neuer Ansatz in der Untersuchung der Zellkernarchitektur. Vorherige Studien besagen, dass Chromosomen keine willkürlichen Positionen im Zellkern einnehmen, sondern sich in spezifischen Territorien, *chromosome territories* (CTs), befinden (Cremer and Cremer 2010). In diesem Kontext konnte gezeigt werden, dass Eigenschaften der Zellkernarchitektur wie die bestimmte Positionierung von Chromosomen im CT oder Bewegungsmechanismen von Chromatin beispielsweise Transkriptionsrate, Zelldifferenzierung oder Zellzyklus beeinflussen (Mehta et al. 2010; Marella et al. 2009; Morey, Kress, and Bickmore 2009). Nachdem Wiener et al. (2010) in einer Studie zu numerischen Chromosomenaberrationen von Chromosom 11 im Plasmozytom der Maus gezeigt haben, dass die Zytobande 11E2 im Telomer des Chromosoms 11 im schnell wachsenden Plasmozytom der Maus verdoppelt ist, stellen wir uns im vorliegenden Zusammenhang die Frage, ob der Faktor Orientierung eine Bedeutung in der Tumorgenese des Plasmozytoms darstellt. Das Plasmozytom ist ein maligner Tumor von Lymphozyten der B-Zell-Reihe und Chromosom 11 Aberrationen stellen eine der häufigsten chromosomalen Aberrationen beim Plasmozytom der Maus dar.

Für die Orientierung des Chromosoms innerhalb des 3D-Zellkerns gibt es unterschiedliche Möglichkeiten. Sowohl das Telomer als auch das zentromernahe Ende des Chromosoms können entweder in Richtung Peripherie oder in Richtung Zentrum zeigen, das Chromosom kann jedoch ebenso parallel zur Zellkernoberfläche liegen, so-

dass kein Ende in Richtung Peripherie oder Zentrum zeigt. Die Orientierung von Chromosomen im 3D-Zellkern wurde bislang noch nie innerhalb einer wissenschaftlichen Studie beurteilt. Dies nachzuholen, war das Ziel unserer Untersuchungen. In Anlehnung an die Studie von Wiener et al. (2010) betrachteten wir hierzu zunächst die Orientierung von Chromosom 11 in normalen B-Lymphozyten und anschließend in Plasmozytomzellen. Im Zentrum beider aus unseren Untersuchungen hervorgegangenen Studien stand die Orientierung von Chromosom 11 in der Interphase im 3D-Nukleus von vier verschiedenen Zelltypen der Maus: Die erste Publikation ("Distinct nuclear orientation patterns for mouse chromosome 11 in normal B lymphocytes") enthält die Ergebnisse der Untersuchung von diploiden Pre-B-Lymphozyten aus BALB/c Mäusen (Pre-B-Zellen) sowie aus primären B-Lymphozyten kongener [T38HxBALB/c]N wildtyp Mäuse (T38Hwt-Lymphozyten); die zweite Publikation ("Changes in Nuclear Orientation Patterns of Chromosome 11 during Mouse Plasmacytoma Development") zeigt die Ergebnisse der Untersuchung von B-Lymphozyten aus [T38HxBALB/c]N Mäusen mit einer reziproken Translokation zwischen den Chromosomen 11 und X (T38HT(X;11)-Lymphozyten), resultierend in einem langen (T(11;X)) und einem kurzen (T(X;11)) Chromosom, sowie von schnell wachsenden Plasmozytomzellen (PCT-Zellen) (Wiener et al.).

Zur Darstellung der beiden homologen Chromosomen 11 im 3D-Nukleus nutzten wir *multicolor banding* (mBANDing) (Benedek et al. 2004). Bei dieser Methode werden vier sich überlappende Regionen des gesamten Chromosoms 11 mit je vier verschiedenen fluoreszierenden Farben dargestellt, sodass die Telomere in grün (FITC), die zentromernahen Enden in magenta (Texas Red) und die subchromosomalen Segmente dazwischen in rot (Gold) und cyan blau (DEAC) sichtbar werden. Pro Zelltyp nahmen wir ca. 300 Nuklei mit einem AxioImager Z2 Mikroskop, entsprechenden Filtern für die vier Fluorochrome und der Software Axiovision 4.8 (Carl Zeiss Inc. Kanada) auf. Mittels visueller Inspektion wurde die Orientierung aller homologen Chromosomen 11 bestimmt.

Die erste Studie ergab als häufigstes Orientierungsmuster sowohl in den Nuklei der Pre-B-Zellen als auch der T38Hwt-Lymphozyten eine parallele Lage beider Chromosomen 11 zur Zellkernoberfläche. Als zweithäufigstes Muster in diesen beiden Gruppen liegt ein Homolog parallel, während das Zweite mit dem Telomer in Richtung Zentrum und mit dem Zentromer in Richtung Peripherie zeigt. Es ließ sich kein signifikanter Unterschied zwischen Pre-B- und T38Hwt-Lymphozyten in Bezug auf ihre Chromosom 11-Orientierungsmuster feststellen ($p>0.05$). Zur Bestätigung dieser Ergebnisse wurde eine semi-automatische quantitative Analyse durchgeführt.

Auch in der zweiten Studie war bei den T38HT(X;11)-Lymphozyten die parallele Lage der beiden Chromosom 11-Homologen zur Zellkernoberfläche das häufigste Orientierungsmuster. Die Plasmozytomzellen zeigten zwei oder mehr Kopien von Chromosom 11. Die beiden Chromosomen 11 von diploiden Zellen zeigten am häufigsten eine parallele Ausrichtung sowie eine Orientierung des Zentromers in Richtung Peripherie beziehungsweise des Telomers in Richtung Zellkernzentrum. Es besteht ein signifikanter Unterschied zwischen den beiden untersuchten Zelltypen dieser Studie in Hinblick auf ihre Orientierungsmuster (p<0.0001). Zusätzlich wurde eine Analyse der diploiden Zellen mit einem vollständig automatischen Programm zur Messung der Orientierung von Chromosomen im 3D-Zellkern (Righolt et al. 2015) durchgeführt.

In der ersten Studie wurde des Weiteren die Formation von Chromosom 11 mittels der Software eADS (Kupper et al. 2007) untersucht. Chromosom 11 zeigte sowohl in Pre-B- als auch in T38Hwt-Zellen eine vorzugsweise gerade, nicht gewinkelte Formation. Zudem wurde eine FACS Analyse der Pre-B- und T38Hwt-Zellen durchgeführt. Sie zeigte, dass sich Pre-B-Lymphozyten über alle Stadien des Zellzyklus verteilen und sich T38Hwt-Lymphozyten bevorzugt in Phase G0/G1 befinden. Dies bedeutet, dass die Orientierung von Chromosom 11 mit hoher Wahrscheinlichkeit unabhängig vom Zellzyklus ist.

Außerdem untersuchten wir in der zweiten Studie die Position des kleinen Translokationschromosoms T(X;11) im 3D-Zellkern. Dieses enthält die Zytobande 11E2 und Teile von E1. Nach *mBANDing* ist es ausschließlich grün (FITC) markiert. Mittels visueller Inspektion wurde festgelegt, ob es sich peripher, zentral oder intermediär befindet. Sowohl in Plasmozytomzellen als auch in T38HT(X;11)-Lymphozyten fand es sich am häufigsten intermediär.

Aus beiden Publikationen wird deutlich, dass es in allen untersuchten Zelltypen eindeutige Orientierungsmuster gibt. Um festzustellen, inwieweit die Veränderungen der Orientierungsmuster während der Plasmozytomentwicklung von Bedeutung sind, bedarf es jedoch weiterer Untersuchungen.

5 My contribution

This cumulative dissertation consists of the two publications “Distinct nuclear orientation patterns for mouse chromosome 11 in normal B lymphocytes” published in BMC Cell Biology in June 2014 and “Changes in nuclear orientation patterns of mouse chromosome 11 during mouse plasmacytoma development” published in Translational Oncology in October 2015.

Prof. Sabine Mai (SMa) from the Institute of Cell Biology, University of Manitoba, Winnipeg, Canada designed both studies. Ann-Kristin Schmälter (AKS) conducted all major experiments independently, discussed the results with SMa and wrote both manuscripts. Dr. Stefan Müller (SMü) and Dr. Christiaan Righolt (CR) were involved in the semi-automatic and automatic analysis. Statistical analysis was done by Mary Cheang from the University of Manitoba. All co-authors were able to incorporate their comments into the manuscripts.

AKS performed cell culture and cell harvest, 2D (metaphase spreads) and 3D (interphase) cell fixation. Alexandra Kuzyk (AK), co-author of both papers, also needed 3D fixed nuclei of these cell types for another study, so a couple of the 3D fixed slides were shared. AKS conducted FISH with a chromosome 11 specific mBAND probe to all 2D and 3D fixed cells and recorded the images.

AKS analyzed all nuclei by visual inspection, determined the orientation of mouse chromosome 11 and the nuclear position of the small translocation chromosome T(X;11). All tables with the results and the representative images shown in both publications were provided by AKS. 3D movies for the supplement of the first publication (“Distinct nuclear orientation patterns for mouse chromosome 11 in normal B lymphocytes”) were created by CR.

AKS prepared the images for the semi-automatic analysis with the software eADS using the program Image J and evaluated the results. SMü and Dr. Michaela Neusser executed the software eADS, analyzed the chromosome 11 conformation and created additional files 13-15 for the first publication (“Distinct nuclear orientation patterns for mouse chromosome 11 in normal B lymphocytes”). The fully automatic program was conducted by CR and AKS controlled whether every chromosome and nucleus was detected correctly by the program. The results of the automatic analysis are discussed in the second publication (“Changes in Nuclear Orientation Patterns of Chromosome 11 during Mouse Plasmacytoma Development”). AK performed FACS analysis.

In conclusion, AKS carried out the main part of all experimental studies and analysis and is first author of both publications.

6 Publication I

Schmälter *et al. BMC Cell Biology* 2014, **15**:22
http://www.biomedcentral.com/1471-2121/15/22

BMC Cell Biology

RESEARCH ARTICLE Open Access

Distinct nuclear orientation patterns for mouse chromosome 11 in normal B lymphocytes

Ann-Kristin Schmälter[1,2], Alexandra Kuzyk[1], Christiaan H Righolt[1,3], Michaela Neusser[2], Ortrud K Steinlein[2], Stefan Müller[2*] and Sabine Mai[1*]

Abstract

Background: Characterizing the nuclear orientation of chromosomes in the three-dimensional (3D) nucleus by multicolor banding (mBANDing) is a new approach towards understanding nuclear organization of chromosome territories. An mBANDing paint is composed of multiple overlapping subchromosomal probes that represent different regions of a single chromosome. In this study, we used it for the analysis of chromosome orientation in 3D interphase nuclei. We determined whether the nuclear orientation of the two chromosome 11 homologs was random or preferential, and if it was conserved between diploid mouse Pre B lymphocytes of BALB/c origin and primary B lymphocytes of congenic [T38HxBALB/c]N wild-type mice. The chromosome orientation was assessed visually and through a semi-automated quantitative analysis of the radial and angular orientation patterns observed in both B cell types.

Results: Our data indicate that there are different preferential patterns of chromosome 11 orientation, which are not significantly different between both mouse cell types ($p > 0.05$). In the most common case for both cell types, both copies of chromosome 11 were oriented in parallel with the nuclear border. The second most common pattern in both types of B lymphocytes was with one homolog of chromosome 11 positioned with its telomeric end towards the nuclear center and with its centromeric end towards the periphery, while the other chromosome 11 was found parallel with the nuclear border. In addition to these two most common orientations present in approximately 50% of nuclei from each cell type, other orientations were observed at lower frequencies.

Conclusions: We conclude that there are probabilistic, non-random orientation patterns for mouse chromosome 11 in the mouse B lymphocytes we investigated ($p < 0.0001$).

Keywords: Chromosome orientation, Three-dimensional nucleus, Nuclear architecture, Fluorescence *in situ* hybridization, Multicolor banding, Chromosome territory

Background

Chromosomes occupy specific regions in the three-dimensional (3D) interphase nucleus, so-called chromosome territories (CTs) [1]. The radial arrangement of CTs shows cell-type specific differences [1,2]. The arrangement of CTs is influenced by many factors, such as chromosome size, gene density and transcription. In lymphocytes, chromosomes with a high gene-density are located further towards the center of the nucleus whereas chromosomes with a lower gene-density are concentrated at the nuclear periphery [1,3-6]. Transcription is also thought to play an important role in CT arrangement, with transcriptionally active genes usually located on the edge or outside of CTs and inactive genes found in the interior [7]. Gene expression can also cause chromatin movement in the 3D nucleus, as active genes may loop out of their CT altogether, presumably to access a transcription factory [8,9]. The correlation between the radial distribution of CTs and factors such as gene density, replication timing and transcription were examined by Küpper et al. [10]. They found that, in human cell nuclei, gene-density has a dominant impact on the radial distribution of CTs. In mouse cell nuclei other factors like

* Correspondence: S.Mueller@lrz.uni-muenchen.de; Sabine.Mai@med.umanitoba.ca
[2]Institute of Human Genetics, University Hospital, Ludwig-Maximilians-University, Goethestr. 29, 80336 Munich, Germany
[1]Manitoba Institute of Cell Biology, University of Manitoba, Cancer Care Manitoba, 675 McDermot Avenue, Winnipeg, Manitoba, Canada
Full list of author information is available at the end of the article

guanine-cytosine content may, however, play a more important role in determining the radial distribution [11].

The position of each CT is established early in G1 and is maintained throughout interphase with minimal constrained diffusion [12]. Changes in the position of CTs have, however, been observed during cell differentiation, senescence and tumorigenesis. This occurs for example during adipocyte [13] and human epidermal keratinocyte differentiation [14]. In human fibroblasts, chromosome positions change when a cell becomes quiescent, senescent or when it re-enters the cell cycle [15,16].

In the present study, we investigated chromosome orientation for the first time in the mouse 3D nucleus. We used multicolor banding (mBANDing). A mBAND paint labels regions of a single chromosome with different fluorochromes. These different stains ensure that the centromeric end, telomeric end and interstitial regions can be differentiated from each other. In the 3D nucleus, the location of each region, and ultimately the orientation of the whole chromosome can, therefore, be determined. mBANDing is commonly used to study intrachromosomal changes in single chromosomes [17], but can also be applied in studies of nuclear architecture. Using mBAND probes, the degree of condensation of human chromosome 5 was determined in both interphase and metaphase [18], more recently the orientation of human chromosomes in sperm nuclei were analyzed [19]. In the latter study, the radial positions of all 24 CTs and their axial *vs.* non-axial as well as their linear *vs.* non-linear, orientations with respect to the sperm tail were determined, as well as the internal organization of chromosome subregions defined by different mBAND probes. A predominantly size-dependent radial arrangement was found for entire CTs. In addition, in particular for the smaller chromosomes, the authors also reported a gene density correlated orientation. Taken together, their study did not identify a preferential internal orientation of CTs with regard to the telomeric and centromeric end.

Our aim was to determine and compare the orientation of chromosome 11 in a diploid mouse PreB lymphocyte cell line and in primary B lymphocytes of congenic [T38HxBALB/c]N wild-type mice. Chromosome 11 is a gene dense chromosome [20]. The mBAND paint labels regions of chromosome 11 with four different fluorochromes. After fluorescence *in situ* hybridization (FISH) on 3D preserved cell nuclei, the location of centromeric, telomeric and interstitial regions and the orientation of chromosome 11 were visually determined for 300 nuclei per cell type. We observed three main patterns of chromosome 11 orientations. One arrangement involved chromosome 11 in parallel with the nuclear border, with neither the telomeric nor centromeric end pointing towards the nuclear center. Alternatively, the telomeric or the centromeric end of chromosome 11 were found pointing towards the nuclear center. Our data show that there is no significant difference between the frequencies of these three patterns of chromosome 11 orientations in both types of mouse B lymphocytes studied.

Results

The mBANDing technique was used to study the nuclear organization of chromosome 11 in a diploid mouse Pre B lymphocyte line of BALB/c origin [21] and in B lymphocytes of congenic [T38HxBALB/c]N wild-type mice [22]. We visualized mBANDed chromosome 11 in metaphase preparations and chromosome territory (CT) 11 in 3D nuclei. Over 300 nuclei of both PreB and [T38HxBALB/c]N wild-type mouse lymphocytes were imaged using Axiovision 4.8 software (Carl Zeiss Inc. Canada). After deconvolution using a constrained iterative algorithm [23], all nuclei were analyzed by visual inspection to determine the orientation of both chromosome 11 homologs. To validate these results, we performed a semi-quantitative analysis of the radial arrangement of individual mBAND probe distributions on a subset of 45 nuclei per cell type using eADS software [10]. The 3D conformation of 90 individual chromosomes 11 from each of the two cell types was determined by measuring angles between the geometric centers of the different mBAND probes in individual chromosome territories. To determine whether cell cycle distribution had an impact on the chromosome 11 orientation patterns seen, cell cycle profiles of both B cell types were measured by FACS analysis.

Chromosome 11 mBANDing in Pre B and T38H wt metaphase preparations

Mouse chromosome 11 is approximately 122 Mb in size and has a mean gene density of 18.7 genes/Mb [24]. The mBAND probe set divides chromosome 11 into four overlapping segments, as illustrated in Figure 1A. The pericentromeric region is labeled with Texas Red, the proximal interstitial region in Gold, the distal interstitial region with DEAC and the telomeric region with FITC, respectively. Hybridization of the chromosome 11 mBAND probe to metaphase spreads (Figure 1B) was performed to examine copy number and structural stability of chromosome 11 in both cell types. Twenty metaphases in three independent FISH experiments were analyzed per cell type. We observed no structural or numerical aberrations in chromosome 11 in the cells studied. Figure 1B represents an example of a PreB lymphocyte metaphase, with both copies of chromosome 11 labeled by the mBAND probe. Figure 1C depicts the mBAND profiles of the two chromosomes from a PreB lymphocyte metaphase. All four fluorochromes can be clearly identified.

mBANDing of chromosome 11 in interphase nuclei

We performed FISH on 3D preserved cell preparations from the two B cell types. With exception for the distal

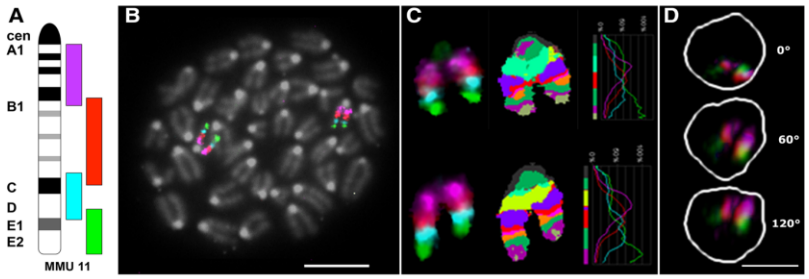

Figure 1 mBAND labeling scheme, metaphase of PreB lymphocytes of BALB/c origin, mBANDed chromosomes 11 and representative [T38HxBALB/c]N wild-type B cell interphase nucleus. A mBAND labeling scheme of mouse chromosome 11. Chromosome 11 is divided into four overlapping segments. Each segment was labeled with a different fluorochrome: the telomeric end in FITC (green), the centromeric end in Texas Red (magenta), and the interstitial segments in DEAC (cyan blue) and Gold (red), respectively. **B** Metaphase from diploid mouse Pre B lymphocytes of BALB/c origin after hybridization with the chromosome 11 mBAND probe. (Scale bar: 10 μm). **C** Two chromosome homologs from a different Pre B lymphocyte metaphase showing (from left to right) display colors, false colors and mBAND fluorescence intensity profiles. **D** Maximum intensity projections of a representative [T38HxBALB/c]N wild-type B cell interphase nucleus, from top to bottom: xy-view (z-projection), 60° and 120° rotation around the y-axis (note: the DEAC labeled probe is not shown because of insufficient signal/noise ratio of the FISH signal. The white line outlines the DAPI stained nucleus). (Scale bars are 5 μm).

interstitial probe labeled with DEAC, all mBAND probes consistently showed the identification of specific FISH signals that were clearly distinguishable from non-specific background. We therefore excluded the DEAC labeled mBAND probe from all further measurements. Image z-stacks from 307 nuclei of PreB and 303 nuclei of [T38HxBALB/c]N wild-type mouse lymphocytes were captured and deconvolved (Materials and Methods). Figure 1D shows a representative chromosome 11 mBANDing image of a [T38HxBALB/c]N wild-type B lymphocyte 3D nucleus. 3D reconstructed images and movies representing various orientation patterns can be viewed in Additional files 1, 2, 3, 4, 5, 6, 7, 8, 9, 10, 11 and 12.

Orientation of chromosome 11 in the 3D nucleus as examined by visual inspection

Using mBANDing, we were able to analyze the chromosome orientation of mouse chromosome 11 subregions for the first time in 3D interphase nuclei. We determined the frequency of nuclear chromosome orientation patterns by visual inspection in all captured nuclei from PreB lymphocytes and [T38HxBALB/c]N wild-type mice. mBAND territories were designated as parallel ("P") to the nuclear surface when no chromosome end was pointing towards the nuclear center or the periphery. A homolog of chromosome 11 was classified as "C" when the centromeric region was localized closest to the nuclear border and "T when its telomeric end showed the most peripheral positioning. Figure 2 provides a cartoon illustration for the various orientation patterns observed. The most frequent pattern observed was with both copies of chromosome 11 located in parallel with the nuclear border ("PP") (37.3% and 31.9%, respectively) (Table 1). There was no significant difference in the occurrence of this orientation pattern between both lymphocyte types against all other patterns combined ($p = 0.20$). The second most common orientation observed was with one homolog of chromosome 11 orientated with its telomeric end pointing towards the nuclear center, while the other chromosome 11 was parallel with the nuclear border ("PC") (20.5% and 26.1% in PreB and [T38HxBALB/c]N wild-type mouse lymphocytes, respectively). There was no significant difference in the frequency of this orientation pattern seen between both types of lymphocytes ($p = 0.13$) (Table 1). One chromosome 11 pointing with its centromeric end to the center and the other in parallel with the nuclear border ("PT") was the third most common orientation we observed. The occurrence of this orientation pattern did not differ significantly in both types of lymphocytes ($p = 0.05$) with a frequency of 16.3% of the PreB nuclei and of 10.4% of the [T38HxBALB/c]N wild-type lymphocyte nuclei (Table 1). In 10.7% of PreB and 5.8% of [T38HxBALB/c]N wild-type lymphocyte nuclei, both copies of chromosome 11 were orientated with their centromeric ends to the nuclear center ("TT") (Table 1). Furthermore, in 9.1% in PreB and 7.3% [T38HxBALB/c]N wild-type lymphocyte nuclei one chromosome 11 pointed towards the nuclear center with its telomeric end and the other points towards the center with its centromeric end ("CT") (Table 1). The scenario that both chromosomes 11 were orientated with their telomeric ends to the nuclear center ("CC") was observed in 6.1% of the PreB and 18.5% of the [T38HxBALB/c]N wild-type mouse lymphocyte nuclei (Table 1).

By visual inspection we observed three main patterns of chromosome 11 orientation in the 3D interphase nucleus: (1) both homologs of chromosome 11 in parallel

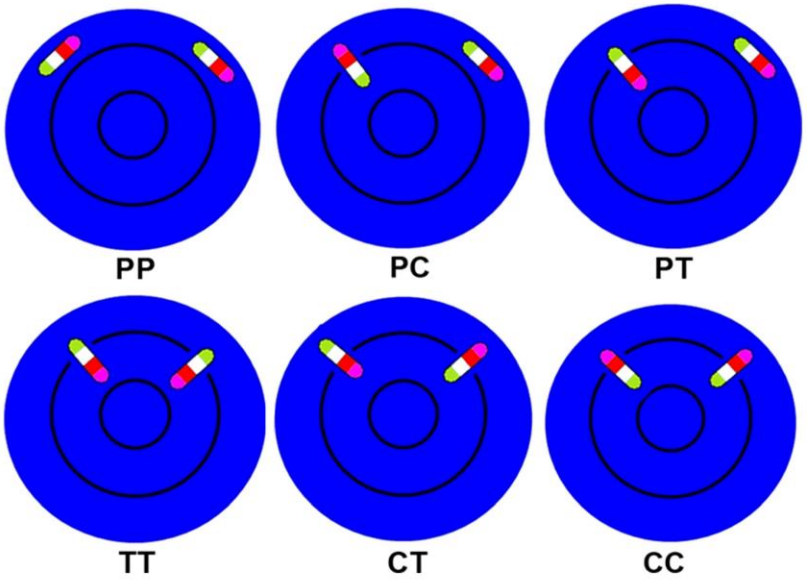

Figure 2 Cartoon illustration of different possibilities of chromosome 11 orientation pairs in the nucleus. The representative chromosome is composed of four differently colored segments; green segments represent telomeric ends, magenta segments centromeric ends, proximal and distal (not measured) interstitial segments are shown in cyan blue and red, respectively. The nucleus is illustrated in blue; the black circles divide the nucleus into central, intermediate and peripheral regions (PP = both homologs parallel to the nuclear periphery, PC/PT = one homolog is located in parallel to the periphery, while the other is oriented with its centromeric (red)/telomeric (green) end towards the nuclear periphery, TT = both homologs point with their telomeric (green) ends towards the periphery, CT = one homolog with its centromeric (red) end and the other homolog with its telomeric (green) end pointing towards the nuclear periphery, CC = both homologs point with their centromeric (red) ends towards the nuclear periphery,). PP, PC and PT in the first row of Figure 2 are observed most frequently.

to the nuclear border ("PP"); (2) one copy of chromosome 11 in parallel to the border and the other copy pointing with its telomeric end towards the nuclear center ("PC"); (3) one copy of chromosome 11 in parallel to the border and the other copy pointing with its centromeric end towards the center ("PT"). Table 1 shows the frequencies of the different orientation patterns in the two cell types and 2x2 chi square *p*-values demonstrating the significant difference of each pattern with respect to all other orientation patterns combined. There was no significant difference in the occurrence of the orientation patterns observed between both B cell types ($p > 0.05$), with the exception of two minor patterns of orientation: when both copies of chromosome 11 pointed with

Table 1 Frequencies of orientation patterns of chromosome 11

	PreB [%]	[T38Hx BALB/c]N wt [%]	Chi-Square [p-value]
Both homologs in parallel to the nuclear border (PP)	37.3	31.9	0.20
One homolog points with its centromere to the nuclear periphery, the other is parallel to the nuclear border (PC)	20.5	26.1	0.13
One copy points with its telomere to the nuclear periphery, the other is parallel to the nuclear border (PT)	16.3	10.4	0.05
Both homologs point with their telomeric end to the nuclear periphery (TT)	10.7	5.8	0.04
One copy points with its telomeric end, and the other copy with centromeric end, to nuclear periphery (CT)	9.1	7.3	0.45
Both copies point with their centromeric ends to the nuclear periphery (CC)	6.1	18.5	<0.0001

Orientation patterns of chromosome 11 and the frequency of orientation in Pre B lymphocytes of BALB/c origin and in B cells of congenic [T38HxBALB/c]N wild-type mice analyzed by visual inspection. A 2x2 Chi-Square test with p-value of >0.05 indicates that the frequency of the orientation is not significantly different between the two cell types. Each pattern was tested between the two cell types against all other patterns combined and the expected values were based on the marginal totals. There is a significant difference in the percentage of cells that display these major 2x3 orientation patterns between the two cell types (p <0.0001). (P = parallel, C = centromere points to periphery, T = telomere points to periphery).

their centromeric ("TT") (p = 0.04) or telomeric ("CC") ($p < 0.0001$) ends towards the nuclear center (Table 1).

A 2x3 contingency analysis of just the three major orientation patterns indicated that there was a significant difference in the distribution of the three patterns between the two cell type ($p < 0.001$).

Semi-automated quantitative analysis of mBAND 11 orientation in mouse lymphocytes

To validate the above results, we analyzed nuclear orientation patterns of individual chromosomes 11 for a subset of 45 nuclei per cell type with the semi-automated software package eADS [9]. The mean radial arrangement of telomeric, interstitial and centromeric mBAND regions was determined in these 45 nuclei from both B cell types. We measured the 3D FISH signal distance to the nuclear surface in nm using eADS software [10], and then transformed these values to relative values (%) by normalizing it to the nuclear radius. Additional files 13, 14, 15 and Additional file 16: Table S1 show the results of the semi-automated software assisted analysis: The data indicate that this semi-quantitative analysis identifies, similar to the visual inspection, three most frequent orientation patterns for mouse chromosome 11.

When comparing the individual results of the quantitative analysis to the analysis by visual inspection of all 45 image per cell type we found, however, that only 30/45 (67%) nuclei of [T38HxBALB/c]N wild-type mouse lymphocyte and 28/45 (62%) nuclei of Pre B lymphocytes showed concordant results with both methods.

3D conformation of mouse chromosome 11

We evaluated the 3D conformation of chromosome 11 in the two lymphocyte cell types using the software eADS [9]. We measured the angles between the geometric centers of centromeric, interstitial and telomeric mBAND territories using the interstitial segment as apex. Analysis of each 90 PreB and [T38HxBALB/c]N wild-type chromosomes using DistAngle software allowed us to determine whether the chromosome territory is preferentially straight or angulated during interphase. Mean measured angles in PreB cells (107°) were very similar compared to [T38HxBALB/c]N wildtype B cells (106°) and showed no statistically significant differences ($p = 0.99$). In both cell types we observed a broad distribution of measured angles (Figure 3A and 3B). 19% of PreB and 15% of [T38HxBALB/c]N wild-type B cell CT11 showed angles between 0 and 60° and were considered as rather angulated. 47% of PreB and 43% of [T38HxBALB/c]N wild-type B cell CT11 showed angles between 121° and 180° and indicate a trend towards a straight configuration (Figure 3A and B).

We also calculated the angle difference between homologous CT11 in individual nuclei. Again, we observed a broad distribution of measured angle differences in both B cell types ranging from 4°-136° (Figure 3C). Mean angle differences between homologs in PreB cells (51°) were slightly larger compared to [T38HxBALB/c]N wild-type B cells (43°), but no statistically significant differences were observed ($p = 0.88$).

Cell cycle profiles

To investigate whether cell cycle stages impact on the nuclear orientation and orientation patterns of mouse chromosome 11, we carried out fluorescent activated cell sorter (FACS) analysis of cell cycle profiles. The DNA profile of the PreB lymphocytes of BALB/c origin is shown in Figure 4A and the DNA profile of the [T38HxBALB/c]N wild-type mouse B cells is shown in Figure 4B. As the PreB lymphocytes were kept proliferating in culture, the cells are distributed throughout the different cell cycle phases with 45.08% in G0/G1, 44.18% in S and 21.80% in G2/M (Figure 4A). Contrastingly, the vast majority of the primary B cells are found in G0/G1 (94.76%) with only 5.22% in S and 2.38% in G2/M (Figure 4B).

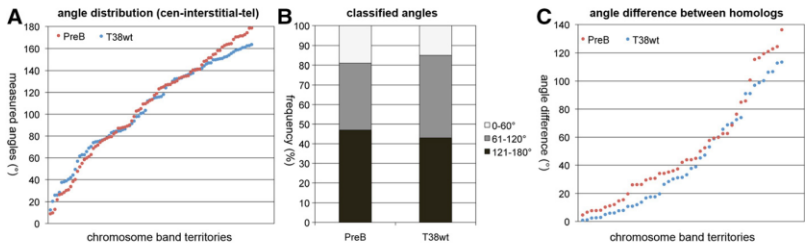

Figure 3 3D conformation analysis of chromosome 11 mBAND territories in Pre B lymphocyte nuclei and in B cell nuclei of congenic [T38HxBALB/c]N wild-type mice using measured angles between geometric centers of centromeric, interstitial (apex) and telomeric chromosome band territories in individual chromosomes A Distribution of measured angles in each 90 PreB and [T38HxBALB/c]N wild-type B individual chromosomes 11. B Bar diagram showing the percentage of angulated chromosomes with telomeric band territories in close proximity to centromeric regions (0-60° = chromosome 11 territory angulated), intermediate (61-120°) and straight chromosomes (121-180° = chromosome 11 territory straight) in the two cell lines. **C** Distribution of calculated angle differences between homologous CT pairs as a measure for the similarity of the 3D conformation of the two chromosomes 11 CT in individual nuclei.

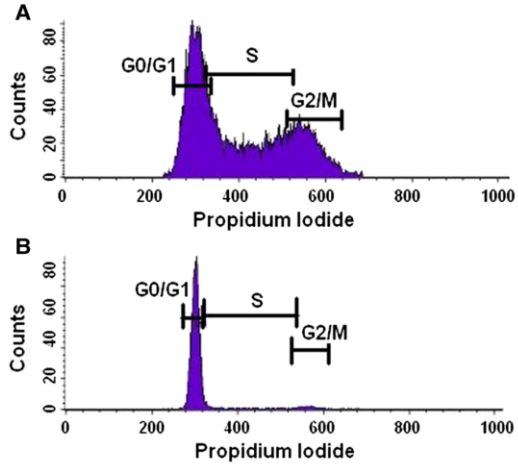

Figure 4 Cell cycle profiles determined by FACS analysis. The graphs illustrate the cell count in the different phases of the cell cycle, which correlates to the propidium iodide intensity. **A** The cell cycle profile of PreB lymphocytes of BALB/c origin. 45.08% of cells are found in G0/G1, 44.18% in S and 21.80% in G2/M. **B** The cell cycle profile of primary B cells from [T38HxBALB/c] wild-type mice. 94.76% of cells are found in G0/G1, 5.22% in s and 2.38% in G2/M.

The comparison of the distinct cell cycle profiles observed for the [T38HxBALB/c]N wild-type mouse B cells and PreB cells indicates that the chromosome 11 orientation is independent of cell cycle profiles in the two B cell types examined in our study.

Discussion

We used mBANDing for the first time to study chromosome orientation in the mouse 3D B cell nucleus. This technique has mostly been used previously to detect intrachromosomal rearrangements such as inversions, translocations and deletions in metaphase spreads [17]. One previous study used mBANDing to examine the spatial arrangements and the 3D configuration of CT in human sperm nuclei, demonstrating that mBANDing is an excellent technique to determine the 3D nuclear orientation of chromosomes [19]. Two alternative approaches were recently described, which could also be applied for a 3D topology analysis of mouse chromosomes, or could even be combined with the mouse mBAND probe set to further enhance the subregional resolution of the FISH banding probe set. One first approach used evolutionary rearranged chromosomes as subchromosomal probes for 3D-FISH [25], the second pooled BAC probes for predefined genomic regions or interest [26].

Using a mouse mBAND 11 probe set, we first determined chromosome 11 orientation by visual inspection. We then conducted a semi-automated quantitative analysis using the software eADS [9]. Both methods agreed on the identification and frequency of three different orientation patterns but did not coincide for each nucleus measured.

This result points to differences in the interpretation of mBAND data by the user (visual inspection) and by the user performing semi-automated analysis that includes the manual segmentation of the regions of interest. During this procedure, some pixels might have been discarded or identified as artifacts when cutting out the bands separately in different channels with no overview of the whole chromosome. It was not possible to distinguish low grey levels from each other or background pixels with value 0, which may lead to mistakes in the manual segmentation. The pixels of the bands were measured with respect to the nucleus stained in DAPI. If DAPI staining was weaker in some cells than in others, then the subsequent identification of the positions of the band pixels are measured inaccurately. Due to the lack of a fully automated program, these current measurements are only indicative of varied chromosome orientation patterns in the cells examined, but no absolute measure of chromosome band positioning. We are currently working towards a fully automated program.

The PreB cells were kept proliferating in culture, while the majority (94.76%) of the primary B cells were directly isolated from the mice (kept under specific pathogen free (SPF) conditions) and are in G0/G1 of the cell cycle; this was confirmed through FACS cell cycle analysis (Figure 4). In cycling PreB cells no correlation was found between cell cycle stage and radial orientation of mBAND CT. We have not determined the cell cycle stage of the individual nuclei, e.g. by BrdU, so we can only state “no difference between cycling and quiescent cells” The influences of differentiation and gene density on the nuclear architecture and on the radial orientation of gene dense telomeric chromatin appear to be a more likely cause for the observed differences between the two cell types. Gene density can be ruled out as cause for differences because it is the same in both cell types. This leaves differentiation as cause, which is linked to transcription.

Transcription may influence chromosome position. Regions of chromatin have been shown to change position in the nucleus with activation and increased levels of transcription [8,27,28]. Transcription factories can also alter the arrangement of chromatin as genes may loop out of their territory to be transcribed [29] or multiple genes will meet to be co-transcribed in a single transcription factory [30]. The access to transcription factories , therefore, may be relevant for the orientation of chromosomes in the nucleus. A possible rotation of a chromosome in the nucleus may be an alternate way in which active regions can access the transcription machinery. For example, chromosome rotation could occur around the centromeric or telomeric end. This would

allow genes that lay close to rotation axis to remain in a stable position whereas those further away will undergo a positional change. Alternatively, or in addition to rotation, a chromosome territory may adopt different large-scale folding patterns in order to reach this goal, which may result in straight or angulated 3D conformations. Additionally, the active state of chromatin with regards to methylation, acetylation and other post-translational histone modifications, may not only alter chromatin condensation but also orientation. To test for the effects of transcription on chromosome orientation was beyond the scope of this study.

In approximately 45% of the nuclei examined, it was observed that the two homologs of chromosome 11 did not have the same orientation. This may be an innate protection mechanism of the cell. It has been shown by Heride et al. [31] that chromosomes are non-randomly closer to a heterologue than a homologue. This led them to propose that it may be evolutionarily important to position chromosomes in this way to avoid homologous recombination and to avoid damaging both copies of a chromosome by a single genotoxic stress event. The same argument may explain why two copies of a chromosome may adopt different orientations in the nucleus.

In this study we examined, for the first time, chromosome orientation in the murine 3D nucleus using mBANDing. We found that the orientation of chromosome 11 in PreB lymphocytes of BALB/c origin and primary B cells of congenic [T38HxBALB/c]N wild-type mice varies between distinct patterns of orientation. Gene density has been thought to be the primary factor influencing lymphocyte CT arrangement. We find, however, that it is not sufficient to determine the orientation of mouse chromosome 11 in B cells. Because gene-density is stable, it cannot account for differences in the three major patterns of chromosome 11 orientation we observed. Although we did not find orientation pattern and gene-density to be linked for chromosome 11 in both B-cell models, this may not hold true for all mouse chromosomes and cell types and should be assessed for other chromosomes and non B lineage cell types. At present, our findings allow us to conclude that chromosomes may display distinct orientations in the interphase nucleus of diploid mouse B cells during some stages of differentiation, but the underlying mechanisms require further investigation.

Conclusion

We analyzed for the first time the orientation of mouse chromosome 11 with respect to the telomeric and centromeric ends of chromosomes in the 3D interphase nucleus. Distinct orientation patterns of CT 11 in PreB lymphocytes of BALB/c origin and primary B cells of congenic [T38HxBALB/c]N wild-type mice were observed. The most frequent pattern was with both homologs positioned in parallel to the nuclear border in both types of B lymphocytes. Alternatively the telomeric or centromeric end was found pointing towards the nuclear periphery or center. Overall, chromosome orientation appears to be a non-random feature of the genome in interphase nuclei.

Methods

Cell harvest and cell culture

Mouse PreB lymphocytes of BALB/c origin [21] were cultured in RPMI 1640 media supplemented with 10% heat-inactivated fetal bovine serum (FBS), 1% penicillin-streptomycin, 1% L-Glutamine, 1% sodium pyruvate and 0.1% β-mercaptoethanol (Invitrogen/Gibco, Burlington, ON, Canada). Cells were incubated at 37°C.

Primary B cells were harvested from spleens of three 6 to 8 weeks old congenic [T38HxBALB/c]N wild-type mice [22]. Procedures were conducted according to Animal Protocol 11-019, approved by Central Animal Care Services, University of Manitoba (Winnipeg, MB, Canada).

2D and 3D fixation

2D chromosome fixation was conducted as described by Mai and Wiener [32]. Primary B cells and PreB lymphocytes were centrifuged for 10 minutes at 1000 rpm. The pellet was resuspended in 0.075 M KCl for 30 minutes. Next the cells underwent centrifugation for 10 minutes at 1000 rpm and then a drop fixation with 3:1 methanol to acetic acid. After resuspension of the pellet, cells were dropped onto slides.

3D nuclei fixation was conducted as described by Solovei et al. [33]. Primary B cells and PreB lymphocytes were centrifuged for 10 minutes at 1000 rpm. After resuspension of the pellet, cells were applied to slides. One hour later, the slides were washed in 1 × phosphate-buffered saline (PBS), 0.3xPBS and then incubated in freshly prepared 3.7% formaldehyde. Next the slides were washed in 0.05% Triton-X-100/1xPBS, followed by a wash in 0.5% Triton-X-100/1xPBS. The slides were then incubated in 20% Glycerol/1×PBS, for at least an hour, and subsequently underwent repeated freeze/thaw cycles in liquid nitrogen. Afterwards, the slides were washed in 0.05% Triton-X-100/1xPBS, followed by incubation in 0.1 M HCl. After washing the slides in 2× saline sodium citrate buffer (SSC) they were kept at least one hour in 50% formamide/2×SSC at 4°C.

Fluorescence-activated cell sorting (FACS) analysis

FACS analysis was conducted as described by Caporali et al. [34]. Briefly, PreB lymphocytes BALB/c origin and primary B cells of [T38HxBALB/c]N wild-type mice were fixed in 70% cold ethanol and incubated at 4°C overnight. The following day, the pellet was washed

twice with 1% FBS in 1xPBS after centrifugation at 1200 rpm for ten minutes. The final pellet was resuspended in 1×PBS and stained with propidium iodide (1 μg/mL) (Sigma Aldrich, Oakville, ON, Canada). Flow cytometry was used to analyze the cell cycle profiles using a FACSCalibur (Becton Dickinson, Mississauga, ON, Canada).

Multicolor banding

The mBANDing probe for mouse chromosome 11 was previously described by Benedek et al. [35] and was purchased from Metasystems (Altussheim, Germany) for the present experiments. The pericentromeric region is labeled with Texas Red, the proximal interstitial region in Gold, the distal interstitial region in DEAC and the telomeric region with FITC, respectively. First, slides were equilibrated in 2×SSC, followed by an RNAase A treatment (100 μg/ml) in 2×SSC for one hour at 37°C, and then incubation in freshly prepared 0.01 M HCl with 100 μg/ml pepsin for two minutes. After washing the slides in 1xPBS, they were pretreated in 1% formaldehyde in 1×PBS/50 mM MgCl2, followed by a wash in 1×PBS. For denaturation, the slides were incubated in 0.1×SSC, and then transferred into 2×SSC at 70°C for 30 minutes. After the solution was cooled down to 37°C, the slides were transferred to 0.1×SSC and then denatured in 0.07 M NaOH at room temperature for one minute. Before dehydration in ethanol (30%, 50%, 70% and 90%), the slides were placed in 0.1×SSC and then 2×SSC at 4°C. Next, the mBANDing probe was applied as recommended, sealed to the slide with rubber cement and incubated for two days at 37°C. Post-hybridization washes included 1×SSC at 75°C and in 4×SSC/0.05% Tween20. The chromatin was counterstained with 4'6'-diamidino-2-phenylindole (DAPI) and mounted with ProLong Gold antifade (Invitrogen/Gibco, Burlington, ON, Canada).

Image acquisition

Two-dimensional image acquisition was performed using an Axioplan 2 microscope (Carl Zeiss Ltd., Toronto, ON, Canada) with a 63x/1.4 oil objective lens (Carl Zeiss Ltd., Toronto, ON, Canada) and the ISIS-FISH imaging system 5.0 SR 3 (Metasystems Group Inc. Boston, MA, USA). A DAPI filter was used to visualize the chromosomal counterstain. To detect the four regions of chromosome 11 that were labeled with different fluorochromes (DEAC, FITC, Gold and TexasRed, respectively), appropriate narrow band pass filters were used (Chroma Technologies). The region pseudo-colored in green was detected by a SP-101 fluorescein isothiocyanate (FITC) filter (Excitation CWL/Bandwidth: 471 nm/39 nm, Emission CWL/Bandwidth: 522 nm/40 nm, Chroma Series No.: SP100), the region pseudo-colored in cyan by a 31036v2 7-diethylaminocoumarin-3-carboxylic acid (DEAC) filter (Excitation CWL/Bandwidth: 436 nm/20 nm, Emission CWL/Bandwidth: 480 nm/30 nm, Chroma Series No.: 31000 Series), the region pseudo-colored in red by a 11006v3 Gold filter (Excitation CWL/Bandwidth: 350 nm/50 nm, Emission CWL/Bandwidth: 515 nm/nm, Chroma Series No.: 11000 Series) and the region pseudo-colored in magenta by a 41004 Texas Red® filter (Excitation CWL/Bandwidth: 560 nm/55 nm, Emission CWL/Bandwidth: 645 nm/75 nm, Chroma Series No.: 41000 Series).

For the 3D image acquisition, an AxioImager Z2 microscope (Carl Zeiss Inc. Canada) equipped with the same filter sets as for 2D image acquisition and an AxioCam MRm (Carl Zeiss Inc. Canada) was used, combined with Axiovision 4.8 software (Carl Zeiss Inc. Canada). To reconstruct a 3D image, z-stacks of 80 slices, with 200 nm axial distance and 102 nm x/y pixel size were acquired. Deconvolution was performed with a constrained iterative algorithm [23] using Axiovision 4.8 software (Carl Zeiss Inc. Canada). The chromosome orientation was determined by visual inspection based on the mBAND FISH pattern.

Quantitative semi-automated analysis

Quantitative measurements of mean radial mBAND probe distributions with respect to the nuclear border were performed using the software eADS, a 3D distance measurement tool described in detail by Küpper et al. [10]. In short, the pixels are manually classified as being band or not and being nucleus or not. The Euclidean distance between the nuclear surface and each bands pixel is then measured from these images. For the probe distributions each pixel in each band is used, for the determination of the orientation only the smallest distance for each band is used. The orientation was determined by the difference in radial position of the telomeric and centromeric band. When the difference was smaller than N percentpoints it was called parallel. The software DistAngle [36] was employed to measure 3D angles between geometric centers of different mBAND probes from individual chromosomes.

Statistical analysis

The different orientations of chromosome 11 were compared to each other and compared between the different types of lymphocytes using all of the following tests: Chi-Square, Likelihood Ratio Chi-Square, Continuity Adj Chi-Square and Mantel Haenszel Chi-Square analysis. The p-values of test results shown here for the comparison of different orientations are the Chi-Square values. All other tests yielded similar results (data not shown).

The Mann-Whitney rank sum test was used to determine statistically significant differences in the median radial arrangement of mBAND FISH signals. A p-value <0.05 was considered significant.

Additional files

Additional file 1: 3D movie of a [T38HxBALB/c]N wild type B cell nucleus with the orientation pattern "CP".

Additional file 2: 3D movie illustrating a Pre B nucleus with the orientation pattern "PP".

Additional file 3: 3D view of a Pre B nucleus with the orientation pattern "CT". One chromosome 11 is oriented with its centromeric end (red) towards the nuclear center, whereas the other chromosome 11 is oriented with its telomeric end (green) towards the center.

Additional file 4: 3D movie illustrating a Pre B nucleus with the orientation pattern "TP".

Additional file 5: 3D view of a Pre B nucleus with the orientation pattern "PP". Both copies of chromosome 11 are located in parallel to the nuclear periphery.

Additional file 6: 3D movie illustrating a Pre B nucleus with the orientation pattern "TT".

Additional file 7: 3D view of a Pre B nucleus with the orientation pattern "TP". One chromosome 11 is oriented with its centromeric end (red) towards the nuclear center and with its telomeric end (green) towards the periphery, the other chromosome is located in parallel to the nuclear periphery.

Additional file 8: 3D movie illustrating a Pre B nucleus with the orientation pattern "CC".

Additional file 9: 3D view of a Pre B nucleus with the orientation pattern "TT". Both copies of chromosome 11 are pointing with their centromeric ends (red) towards the nuclear center, whereas their telomeric ends (green) are pointing towards the periphery.

Additional file 10: 3D view of a [T38HxBALB/c]N wild type B cell nucleus with the orientation pattern "CP". One chromosome 11 is located in parallel to the nuclear periphery, the other is oriented with its telomeric end (green) towards the center.

Additional file 11: 3D movie of a [T38HxBALB/c]N wild type B cell nucleus with the orientation pattern "CP".

Additional file 12: 3D view of a [T38HxBALB/c]N wild type B cell nucleus with the orientation pattern "CC". Both copies of chromosome 11 are pointing with their telomeric ends (green) towards the nuclear center.

Additional file 13: Mean radial distribution of the centromeric, interstitial and telomeric mBAND FISH signals in A PreB and B T38wt cell nuclei. The 3D FISH signal distance to the nuclear surface was measured nm using eADS software (Küpper et al., 2007) (n = number of nuclei, nm = nanometer). **A** In PreB cells the mean radial position of the telomeric segment was at 2016 nm and 42% relative distance from the nuclear surface, the interstitial segment at 2178 nm (46%) and the centromeric segment at 2151 nm (45%). **B** In T38wt cells mean absolute and relative probe distances to nuclear surface were 1906 nm (56%) for the telomeric region, 1617 nm (47%) for the interstitial and 1522 nm (44%) for the centromeric region. A small percentage of nuclei shows band signals beyond the nuclear border. This is probably due to weak nuclear DAPI stain measured by the software eADS (see Discussion).

Additional file 14: Normalized (% distance to nuclear surface) radial centromeric, interstitial and telomeric mBAND probe distributions in individual chromosomes from each 45 A PreB and B [T38HxBALB/c]N wild-type B cell nuclei using eADS software. The 3D FISH signal distance to the nuclear surface in nm was transformed to relative values (%) by normalization using the nuclear radius as reference. Each colored dot represents the radial position of the geometric center from an individual chromosome 11. The two chromosome 11 homologs from each nucleus are shown side by side. Nuclei with a similar radial orientation of the two homologs are depicted in clusters separated by bold vertical lines. mBAND territories were designated as parallel ("P") to the nuclear surface when each of the measured relative radial distances between centromeric, telomeric and interstitial chromosome segments was less than 15% of the nuclear radius. This equals to approximately a 400-500 nm radial distance depending on the size of the respective nucleus. We chose a 15% cut-off level because this is approximately twice the distance between consecutive image z-sections of 200 nm. Consequently, in chromosome 11 territories where at least one of the measured relative distances between mBAND territories would exceed 15% the CT was assigned an orientation with either the telomeric or the interstitial or the centromeric end pointing towards the nuclear periphery or center. (P = parallel, C = centromere points to periphery, I = interstitial is most peripheric, T = telomere points to periphery).

Additional file 15: Relative radial orientation of 45 homologous chromosome 11 mBAND CT pairs from each 45 PreB and [T38HxBALB/c]N wildtype B cell interphase nuclei. Frequencies (%) of homologous CT pairs showing different combinations of radial orientations. (P = parallel, C = centromere points to periphery, I = interstitial is most peripheric, T = telomere points to periphery).

Additional file 16: Table S1. Results of semi-automated quantitative analysis using the software eADS. Frequencies of relative orientation patterns of homologous chromosomes in individual nuclei. (P=parallel, C=centromere points to periphery, I=interstitial is most peripheric, T=telomere points to periphery).

Abbreviations

2D: Two-dimensional; 3D: Three-dimensional; CT: Chromosome territory; DAPI: 4'6'-diamidino-2-phenylindole; DEAC: 7-diethylaminocoumarin-3-carboxylic acid; FACS: Fluorescence-activated cell sorting; FISH: Fluorescent *in situ* hybridization; FITC: Fluorescein isothiocyanate; FBS: Fetal bovine serum; mBANDing: Multicolor banding; PBS: Phosphate-buffered saline; SSC: Saline sodium citrate buffer.

Competing interests

The authors declare that they have no competing interests.

Author's contribution

AKS carried out 2D and 3D cell preparation and fixation, mBANDing, image acquisition, visual inspection, conducted the analysis by the software eADs and drafted the manuscript. AK contributed to FACS, contributed to 2D and 3D fixation of cells and to the writing of the manuscript. CR contributed to the discussion, created 3D movies, assisted in data analysis and contributed to writing the manuscript. MN participated in the analysis by eADS. OS is AKS' co-supervisor. SMü conducted the analysis by eADS and contributed to writing the paper. SMa designed the study and helped to draft the manuscript. All authors read and approved the final manuscript.

Acknowledgements

This study was supported by CIHR. AKS received a travel award from Bayer. We thank Mary Cheang for statistical analysis and Dr. Ludger Klewes for his help with FACS analysis.

Author details

[1]Manitoba Institute of Cell Biology, University of Manitoba, Cancer Care Manitoba, 675 McDermot Avenue, Winnipeg, Manitoba, Canada. [2]Institute of Human Genetics, University Hospital, Ludwig-Maximilians-University, Goethestr. 29, 80336 Munich, Germany. [3]Department of Imaging Physics, Delft University of Technology, Delft, The Netherlands.

Received: 4 September 2013 Accepted: 30 May 2014
Published: 12 June 2014

References

1. Cremer T, Cremer M: **Chromosome territories.** *Cold Spring Harb Perspect Biol* 2010, **2**(3):a003889.
2. Bolzer A, Kreth G, Solovei I, Koehler D, Saracoglu K, Fauth C, Muller S, Eils R, Cremer C, Speicher MR, Cremer T: **Three-dimensional maps of all chromosomes in human male fibroblast nuclei and prometaphase rosettes.** *PLoS Biol* 2005, **3**(5):e157.
3. Croft JA, Bridger JM, Boyle S, Perry P, Teague P, Bickmore WA: **Differences in the localization and morphology of chromosomes in the human nucleus.** *J Cell Biol* 1999, **145**(6):1119–1131.
4. Boyle S, Gilchrist S, Bridger JM, Mahy NL, Ellis JA, Bickmore WA: **The spatial organization of human chromosomes within the nuclei of normal and emerin-mutant cells.** *Hum Mol Genet* 2001, **10**(3):211–219.

5. Tanabe H, Habermann FA, Solovei I, Cremer M, Cremer T: **Non-random radial arrangements of interphase chromosome territories: evolutionary considerations and functional implications.** *Mutat Res* 2002, **504**(1–2):37–45.
6. Saccone S, Federico C, Bernardi G: **Localization of the gene-richest and the gene-poorest isochores in the interphase nuclei of mammals and birds.** *Gene* 2002, **300**(1–2):169–178.
7. Morey C, Kress C, Bickmore WA: **Lack of bystander activation shows that localization exterior to chromosome territories is not sufficient to up-regulate gene expression.** *Genome Res* 2009, **19**(7):1184–1194.
8. Lanctot C, Cheutin T, Cremer M, Cavalli G, Cremer T: **Dynamic genome architecture in the nuclear space: regulation of gene expression in three dimensions.** *Nat Rev Genet* 2007, **8**(2):104–115.
9. Sutherland H, Bickmore WA: **Transcription factories: gene expression in unions?** *Nat Rev Genet* 2009, **10**(7):457–466.
10. Kupper K, Kolbl A, Biener D, Dittrich S, von Hase J, Thormeyer T, Fiegler H, Carter NP, Speicher MR, Cremer T, Cremer M: **Radial chromatin positioning is shaped by local gene density, not by gene expression.** *Chromosoma* 2007, **116**(3):285–306.
11. Hepperger C, Mannes A, Merz J, Peters J, Dietzel S: **Three-dimensional positioning of genes in mouse cell nuclei.** *Chromosoma* 2008, **117**(6):535–551.
12. Thomson I, Gilchrist S, Bickmore WA, Chubb JR: **The radial positioning of chromatin is not inherited through mitosis but is established de novo in early G1.** *Curr Biol* 2004, **14**(2):166–172.
13. Kuroda M, Tanabe H, Yoshida K, Oikawa K, Saito A, Kiyuna T, Mizusawa H, Mukai K: **Alteration of chromosome positioning during adipocyte differentiation.** *J Cell Sci* 2004, **117**(Pt 24):5897–5903.
14. Marella NV, Seifert B, Nagarajan P, Sinha S, Berezney R: **Chromosomal rearrangements during human epidermal keratinocyte differentiation.** *J Cell Physiol* 2009, **221**(1):139–146.
15. Bridger JM, Boyle S, Kill IR, Bickmore WA: **Re-modelling of nuclear architecture in quiescent and senescent human fibroblasts.** *Curr Biol* 2000, **10**(3):149–152.
16. Mehta IS, Amira M, Harvey AJ, Bridger JM: **Rapid chromosome territory relocation by nuclear motor activity in response to serum removal in primary human fibroblasts.** *Genome Biol* 2010, **11**(1):R5.
17. Chudoba I, Plesch A, Lorch T, Lemke J, Claussen U, Senger G: **High resolution multicolor-banding: a new technique for refined FISH analysis of human chromosomes.** *Cytogenet Cell Genet* 1999, **84**(3–4):156–160.
18. Lemke J, Claussen J, Michel S, Chudoba I, Muhlig P, Westermann M, Sperling K, Rubtsov N, Grummt UW, Ullmann P, Kromeyer-Hauschild K, Liehr T, Claussen U: **The DNA-based structure of human chromosome 5 in interphase.** *Am J Hum Genet* 2002, **71**(5):1051–1059.
19. Manvelyan M, Hunstig F, Bhatt S, Mrasek K, Pellestor F, Weise A, Simonyan I, Aroutiounian R, Liehr T: **Chromosome distribution in human sperm - a 3D multicolor banding-study.** *Mol Cytogenet* 2008, **1**:25.
20. Sakharkar MK, Perumal BS, Sakharkar KR, Kangueane P: **An analysis on gene architecture in human and mouse genomes.** *In Silico Biol* 2005, **5**(4):347–365.
21. Mai S, Hanley-Hyde J, Rainey GJ, Kuschak TI, Paul JT, Littlewood TD, Mischak H, Stevens LM, Henderson DW, Mushinski JF: **Chromosomal and extrachromosomal instability of the cyclin D2 gene is induced by Myc overexpression.** *Neoplasia* 1999, **1**(3):241–252.
22. Wiener F, Schmalter AK, Mowat MR, Mai S: **Duplication of Subcytoband 11E2 of chromosome 11 is regularly associated with accelerated tumor development in v-abl/myc-Induced Mouse Plasmacytomas.** *Genes Cancer* 2010, **1**(8):847–858.
23. Schaefer LH, Schuster D, Herz H: **Generalized approach for accelerated maximum likelihood based image restoration applied to three-dimensional fluorescence microscopy.** *J Microsc* 2001, **204**(Pt 2):99–107.
24. **Genome reference consortium mouse build 38.** http://www.ncbi.nlm.nih.gov/assembly/GCF_000001635.20/.
25. Neusser M, Schubel V, Koch A, Cremer T, Muller S: **Evolutionarily conserved, cell type and species-specific higher order chromatin arrangements in interphase nuclei of primates.** *Chromosoma* 2007, **116**(3):307–320.
26. Teller K, Illner D, Thamm S, Casas-Delucchi CS, Versteeg R, Indemans M, Cremer T, Cremer M: **A top-down analysis of Xa- and Xi-territories reveals differences of higher order structure at >/=20 Mb genomic length scales.** *Nucleus* 2011, **2**(5):465–477.
27. Chuang CH, Carpenter AE, Fuchsova B, Johnson T, de Lanerolle P, Belmont AS: **Long-range directional movement of an interphase chromosome site.** *Curr Biol* 2006, **16**(8):825–831.
28. Akhtar A, Gasser SM: **The nuclear envelope and transcriptional control.** *Nat Rev Genet* 2007, **8**(7):507–517.
29. Volpi EV, Chevret E, Jones T, Vatcheva R, Williamson J, Beck S, Campbell RD, Goldsworthy M, Powis SH, Ragoussis J, Trowsdale J, Sheer D: **Large-scale chromatin organization of the major histocompatibility complex and other regions of human chromosome 6 and its response to interferon in interphase nuclei.** *J Cell Sci* 2000, **113**(Pt 9):1565–1576.
30. Osborne CS, Chakalova L, Mitchell JA, Horton A, Wood AL, Bolland DJ, Corcoran AE, Fraser P: **Myc dynamically and preferentially relocates to a transcription factory occupied by Igh.** *PLoS Biol* 2007, **5**(8):e192.
31. Heride C, Ricoul M, Kieu K, von Hase J, Guillemot V, Cremer C, Dubrana K, Sabatier L: **Distance between homologous chromosomes results from chromosome positioning constraints.** *J Cell Sci* 2010, **123**(Pt 23):4063–4075.
32. Mai S, Wiener F: **The impact of p53 loss on murine plasmacytoma development.** *Chromosome Res* 2002, **10**(3):239–251.
33. Solovei I, Cavallo A, Schermelleh L, Jaunin F, Scasselati C, Cmarko D, Cremer C, Fakan S, Cremer T: **Spatial preservation of nuclear chromatin architecture during three-dimensional fluorescence in situ hybridization (3D-FISH).** *Exp Cell Res* 2002, **276**(1):10–23.
34. Caporali A, Wark L, Vermolen BJ, Garini Y, Mai S: **Telomeric aggregates and end-to-end chromosomal fusions require myc box II.** *Oncogene* 2007, **26**(10):1398–1406.
35. Benedek K, Chudoba I, Klein G, Wiener F, Mai S: **Rearrangements of the telomeric region of mouse chromosome 11 in Pre-B ABL/MYC cells revealed by mBANDing, spectral karyotyping, and fluorescence in-situ hybridization with a subtelomeric probe.** *Chromosome Res* 2004, **12**(8):777–785.
36. Grasser F, Neusser M, Fiegler H, Thormeyer T, Cremer M, Carter NP, Cremer T, Muller S: **Replication-timing-correlated spatial chromatin arrangements in cancer and in primate interphase nuclei.** *J Cell Sci* 2008, **121**(Pt 11):1876–1886.

doi:10.1186/1471-2121-15-22
Cite this article as: Schmälter *et al.*: Distinct nuclear orientation patterns for mouse chromosome 11 in normal B lymphocytes. *BMC Cell Biology* 2014 **15**:22.

7 Publication II

Translational Oncology
www.transonc.com

Volume 8 Number 5 October 2015 pp. 417–423 417

Changes in Nuclear Orientation Patterns of Chromosome 11 during Mouse Plasmacytoma Development[1]

Ann-Kristin Schmälter*,†, Christiaan H. Righolt*,‡, Alexandra Kuzyk*, and Sabine Mai*

*Manitoba Institute of Cell Biology, University of Manitoba, CancerCare Manitoba, Winnipeg, MB, Canada
†Institute of Human Genetics, University Hospital, Ludwig-Maximilians-University, Munich, Germany;
‡Department of Imaging Physics, Delft University of Technology, Delft, The Netherlands

Abstract

Studying changes in nuclear architecture is a unique approach toward the understanding of nuclear remodeling during tumor development. One aspect of nuclear architecture is the orientation of chromosomes in the three-dimensional nuclear space. We studied mouse chromosome 11 in lymphocytes of [T38HxBALB/c]N mice with a reciprocal translocation between chromosome X and 11 (T38HT(X;11)) exhibiting a long chromosome T(11;X) and a short chromosome T(X;11) and in fast-onset plasmacytomas (PCTs) induced in the same strain. We determined the three-dimensional orientation of chromosome 11 using a mouse chromosome 11 specific multicolor banding probe. We also examined the nuclear position of the small translocation chromosome T(X;11) which contains cytoband 11E2 and parts of E1. Chromosomes can point either with their centromeric or with their telomeric end toward the nuclear center or periphery, or their position is found in parallel to the nuclear border. In T38HT(X;11) nuclei, the most frequently observed orientation pattern was with both chromosomes 11 in parallel to the nuclear border ("PP"). PCT cells showed nuclei with two or more copies of chromosome 11. In PCTs, the most frequent orientation pattern was with one chromosome in parallel and the other pointing with its centromeric end toward the nuclear periphery ("CP"). There is a significant difference between the orientation patterns observed in T38HT(X;11) and in PCT nuclei ($P < .0001$).

Translational Oncology (2015) 8, 417–423

Introduction

Chromosomes are organized in evolutionary conserved chromosome territories [1]. Their nonrandom three-dimensional (3D) positions were previously described [2], e.g., the localization of the active and inactive chromosome X and their respective genes [3,4]. Euchromatin of rod photoreceptor cells in nocturnal mammals is found in the periphery, whereas it is found in the center in diurnal mammals [5]. Not only chromosome territories are in the focus of research but also the localization of telomeric regions [6,7].

Tumor development is greatly influenced by genomic instability [8], and telomere dysfunction plays an important role in genomic instability [9]. Therefore, it is essential to study nuclear architecture in normal and tumor cells. Movement of telomeric regions during the cell cycle was observed in living ECV-TRF1 and -TRF2 cells [10] and in human osteosarcoma U2OS cells [11]. Chromosomes of primary human fibroblasts alter their positions within 15 minutes after they are made quiescent due to a removal of serum from the culture medium. This repositioning is probably dependent on nuclear myosin 1β [12]. Further changes of chromosome positions can be found during adipocyte differentiation [13] or T-cell differentiation [14].

Telomere lengthening is a method to prevent genomic instability of rapidly dividing cells [15]. This can occur due to telomerase [16] or due to cycles of homologous recombination during the process of

Address all correspondence to: Sabine Mai, Manitoba Institute of Cell Biology, 675 McDermot Ave, Winnipeg MB R3E0V9, Canada.
E-mail: sabine.mai@umanitoba.ca
[1] This study was supported by the Canadian Institutes of Health Research.
Received 28 April 2015; Revised 15 September 2015; Accepted 15 September 2015

1936-5233/15
http://dx.doi.org/10.1016/j.tranon.2015.09.001

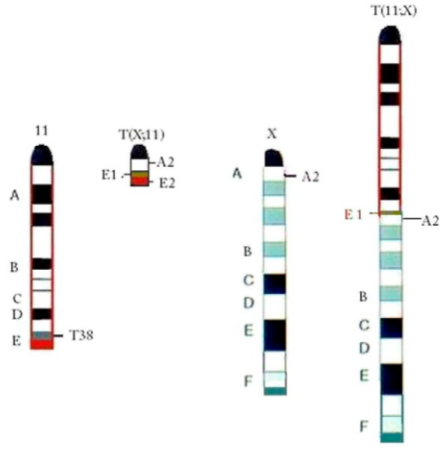

Figure 1. Graphical illustration of the chromosomal constitution of chromosomes 11 in the (BALB/c x T38H) F1 N backcross generation mouse. Chromosome (Chr) 11 with the breakpoint T38H in the telomeric cytoband 11E1 (brown), while the breakpoint in Chr X is located in the centromeric A2 band. The cytoband 11 E2 is colored in red. The reciprocally translocted T(11;X) chromosome resulted from the fusion of the ABCD bands of Chr 11 proximal to the T38H breakpoint with the centromeric A2 band of Chr X. The T(X;11) chromosome was generated by the translocation of the X-derived A2 sub-band onto the 11E1 cytoband of Chr 11. This figure has been published in *Genes Cancer*. 2010;1(8):847–858 [19] and is reprinted here with permission.

alternative telomere lengthening [17]. In fast-onset plasmacytomas (PCTs), the telomere length is significantly increased for the translocation chromosome T(X;11) carrying 11E2 [18].

In the current study, we used a [T38HxBALB/c]N congenic mouse model with a reciprocal translocation between chromosomes X and 11 (rcpT(X;11). This unique mouse model exhibits a long chromosome T(11;X) and a short chromosome T(X;11). The short chromosome T(X;11) contains cytoband 11E2 and parts of cytoband E1 (Figure 1) [19]. To determine the chromosome orientation in cancer cells and in the same cell lineage, we studied mouse PCT induced in this unique mouse model. There are slow- and fast-developing PCTs. Slow-onset PCTs are induced only by pristane (2,6,10,14-tetramethylpentadecane) [20]; fast-onset PCTs are induced by pristane and *v-abl/myc* [19,21]. In the current study, we focused on the fast-onset PCTs. These exhibit a nonrandom duplication of chromosome 11, cytoband 11E2, associated with the overexpression of genes within 11E2 [19]. Cytoband 11E2 is syntenic to human chromosome 17q25 and rat 10q32 [22]. It is frequently altered in tumors of lymphoid and nonlymphoid origin [23–25]. The mean latency of fast-onset PCTs is only 45 days [19,21]. We compared these fast-onset PCT cells with control B lymphocytes of [T38HxBALB/c]N mice with the rcpT(X;11) translocation (T38HT(X;11)).

Our aim was to determine the orientation of chromosome 11 in PCTs and lymphocytes of [T38HxBALB/c]N rcpT(X;11) mice. In a previous study, we determined the orientation of chromosome 11 in 3D nuclei of PreB lymphocytes of BALB/c origin and of [T38HxBALB/c]N wild-type mice without the rcpT(X;11) translocation [26] and found a distinct difference between the frequency of the observed orientation patterns in both cell types. Both normal lymphocyte types studied showed a preference in chromosome 11 orientation, where both chromosomes 11 were observed in parallel to the nuclear border [26]. In the current study, we investigated potential changes in the orientation that occur during the process of PCT development.

Originally, multicolor banding (mBANDing) was developed to detect intrachromosomal changes in metaphases [27]. In our previous study, we used mBANDing for the first time in 3D interphase nuclei to determine the orientation of chromosome 11. Chromosome 11 is labeled by four overlapping fluorochromes (Texas Red, GOLD, DEAC, and FITC). This enabled us to analyze whether the centromeric or the telomeric end was orientated toward the nuclear center or periphery. Only one other group used mBANDing on interphase nuclei before. They studied the grade of condensation of human chromosome 5 [28].

We analyzed the orientation patterns of chromosome 11 in PCT cells and [T38HxBALB/c]N rcpT(X;11) lymphocytes. There was a significant difference noted with respect to their chromosome 11 orientation ($P < .0001$). The nuclear position of the small translocation T(X;11) was also studied visually. It was most frequently found in the intermediate region of the nucleus. There was no significant change in position of T(X;11) detected between the two cell types ($P = .06$).

Material and Methods

Cell Harvest

Primary lymphocytes were harvested from spleens of 6- to 8-week-old congenic [T38HxBALB/c]N rcpT(X;11) mice [19]. PCT cells were harvested from the ascites of fast-onset PCT mice. The [T38HxBALB/c]N rcpT(X;11) mice were pretreated with pristane intraperitoneally and after 5 days infected with a *v-abl/myc* virus also administered intraperitoneally. The mean latency of fast-onset PCTs is 45 days [19,21]. Procedures were performed in accordance to Animal Protocol 11-019 approved by Central Animal Care Services, University of Manitoba (Winnipeg, MB, Canada).

3D Nuclear Hybridizations

For 3D nuclei fixation, lymphocytes were centrifuged at 1000 rpm for 10 minutes. After resuspension of the pellet, cells were carefully placed onto slides and fixed with 3.7% formaldehyde/1 × PBS for 20 minutes at room temperature. Next, the slides underwent washing steps in 1 × PBS shaking. Subsequently, the slides were washed in 0.5% Triton-X-100 for 10 minutes. The slides were incubated for 1 to 2 hours in 20% glycerol and were then subjected to four freeze-thaw cycles in liquid nitrogen afterward. Next, the slides were washed 3 × in 1 × PBS and then incubated in fresh 0.1 M HCl for 5 minutes. After washing the slides in 1 × PBS, they were placed for at least 1 hour in 70% formamide/2 × SSC.

Multicolor Banding

The mBANDing probe for mouse chromosome 11 (Metasystems, Altussheim, Germany) was developed by Benedek et al. (2004) [29]. The slides were equilibrated in 2 × SSC, treated with RNAase A (100 μg/ml) in 2 × SSC at 37°C for 1 hour, and then incubated in freshly prepared 0.01 M HCl with 100 μg/ml pepsin for 2 minutes. After washing the slides in 1 × PBS, they were pretreated in 1% formaldehyde in 1 × PBS/50 mM $MgCl_2$, followed by washing in 1 × PBS. Next, the slides were incubated in 0.1 × SSC and then

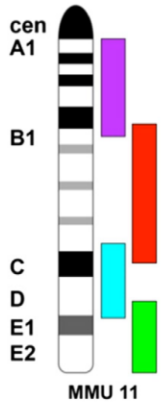

Figure 2. mBAND labeling scheme of mouse chromosome 11. Mouse chromosome 11 is divided into four overlapping segments. The telomeric end is labeled with FITC (green), the centromeric end with Texas Red (magenta), and the intermediate bands with DEAC (cyan blue) and Gold (red). Note cytoband 11E2 at the telomeric end. This figure has been published in *BMC Cell Biology* 2014, 15:22 http://dx.doi.org/10.1186/1471-2121-15-22 [26] and is reprinted here with permission.

transferred into 2× SSC at 70°C for 30 minutes for denaturation. After cooling the solution to 37°C, the slides were transferred to 0.1× SSC and then subjected to 0.07 M NaOH at room temperature for 1 minute. Afterward, the slides were placed in 0.1× SSC and then 2× SSC at 4°C followed by dehydration in ethanol (30%, 50%, 70%, and 90%). Next, the mBANDing probe was applied. The slides were sealed with rubber cement and incubated for 2 days at 37°C. After hybridization, the slides were washed in 1× SSC at 75°C and in 4× SSC/0.05% Tween20. The cells were counterstained with 4'6'-diamidino-2-phenylindole and mounted with ProLong Gold antifade (Invitrogen/Gibco, Burlington, ON, Canada).

Image Acquisition

For the two-dimensional image acquisition, an Axioplan 2 microscope (Carl Zeiss Ltd., Toronto, ON, Canada) with a 63×/1.4 oil objective lens (Carl Zeiss Ltd., Toronto, ON, Canada) and the ISIS-FISH imaging system 5.0 SR 3 (Metasystems Group Inc., Boston, MA) were used. The chromosomal counterstain was visualized with the help of a 4'6'-diamidino-2-phenylindole filter. To detect the four regions of chromosome 11 that were labeled with different fluorochromes (DEAC, FITC, Gold, and Texas Red), narrow band-pass filters were used (Chroma Technologies) as described by our group previously.

3D image acquisition was conducted using an AxioImager Z2 microscope (Carl Zeiss Inc. Canada) equipped with the same filters and an AxioCam MRm (Carl Zeiss Inc. Canada), combined with the Axiovision Release 4.8 software (Carl Zeiss Inc. Canada). Z-stacks of 80 slices, with 200-nm axial distance and 102-nm lateral pixel size, were acquired to reconstruct a 3D image. Using Axiovision Release 4.8 software (Carl Zeiss Inc. Canada), deconvolution was conducted with the constrained iterative algorithm (Schaefer et al., 2001).

Image Analysis

The results presented in this paper were analyzed by visual inspection. The chromosome 11 mBAND probe is composed of four different fluorochromes labeling four different overlapping regions of

Table 1. Orientation Patterns of Chromosome 11 and Their Frequency in Diploid Cells of Congenic [T38HxBALB/c]N Mice Showing T(X;11) and in PCTs

	T38H T[X;11]	Diploid PCTs	Triploid PCTs	Tetraploid PCTs	All PCTs
Both homologs in parallel to the nuclear border (PP)	90	24			24
One copy points with telomeric end to the nuclear center; the other copy is in parallel (PT)	35	19			19
Both homologs point with their telomeric end to the nuclear periphery (TT)	8	7			7
One copy points with its telomeric end and the other copy with its centromeric end to the nuclear periphery (CT)	15	7			7
Both copies point with their centromeric ends to the nuclear periphery (CC)	48	13			13
One homolog points with its centromere to the nuclear periphery; the other is parallel to the nuclear border (CP)	61	30			30
CCC			1		1
CCP			8		8
CPP			12		12
CPT			19		19
CCT			9		9
CTT			2		2
TTT			2		2
PTT			7		7
PPT			15		15
PPP			17		17
CCCP				1	1
CCPP				4	4
CPPP				4	4
PPPP				5	5
CPPT				3	3
CPTT				3	3
CCPT				3	3
PPTT				3	3
PPPT				5	5
PTTT				1	1

The table shows the orientation patterns observed in the diploid T38HT(X;11) cells and in PCTs with two, three, or four copies of chromosome 11. The last column lists the orientation patterns in all PCT cells together (C = centromere points to periphery, T = telomere points to periphery, P = chromosome is parallel to nuclear periphery).

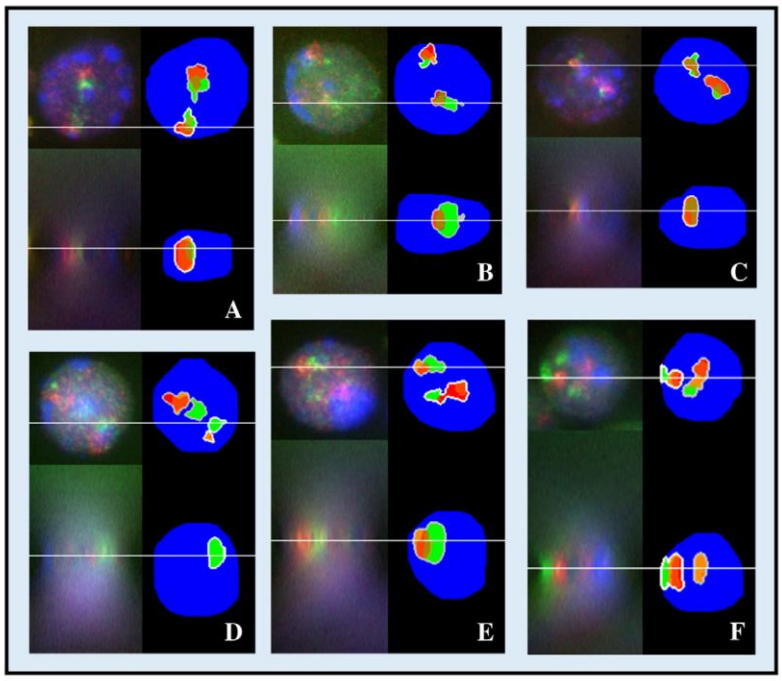

Figure 3. 3D images of diploid PCT and T38HT(X;11) nuclei analyzed by the automatic program (C = centromere (magenta) points to periphery, T = telomere (green) points to periphery). The acquired nuclei, respectively, the same nuclei demonstrated with false colors after segmentation, are displayed in the *xy*-axis (at the top) and in the *xz*-axis (at the bottom). (A) PCT nucleus showing the orientation "CC." (B) PCT nucleus with the orientation pattern "CT." (C) PCT nucleus showing the orientation pattern "TT." (D) T38HT(X;11) nucleus showing the orientation "CC." (E) T38HT(X;11) nucleus with the orientation pattern "CT." (F) T38HT(X;11) nucleus showing the orientation pattern "TT."

the whole chromosome 11. The telomeric end is labeled with FITC (green), the centromeric end with Texas Red (magenta), and the intermediate bands with DEAC (cyan blue) and Gold (red) (Figure 2). DEAC was not always detectable. The mBAND paint made it possible for the visual observer to determine the orientation of chromosome 11. To analyze the position of the small translocation chromosome T(X;11) labeled only with FITC (green), we divided the nucleus visually into three regions: periphery, intermediate, and center.

In addition, we used novel automated software to confirm our visual results [30]. In short, the nucleus was segmented first with an isodata threshold after some smoothing and out-of-focus blur subtraction. The chromosome bands were then segmented after the recorded images were blurred based on the band sizes. These bands were then linked together to chromosome territories based on a utility function determined by overlap and distance between the segmented bands. The orientation of each CT was then determined by calculating the eigenvectors of the inertia tensor; the orientation is indicated by the more outlying band. Consequently, the chromosome is pointing either with its telomeric end or with its centromeric end toward the nuclear periphery. Because an exact measurement is performed, no parallel orientation category is needed anymore.

The automatic analysis was only performed for the diploid cells. Automation of chromosome orientation by this program was not implemented for tri- and tetraploid cells. Therefore, we present the results assessed by visual inspection. Over 300 nuclei per cell type were acquired, and we were able to determine the orientation pattern in 224 PCT and 257 T38HT(X;11) nuclei.

Statistical Analysis

The visually assessed orientation patterns were analyzed by chi-square, likelihood ratio chi-square, and Mantel-Haenszel chi-square tests. The nuclear positions of T(X;11) were compared by the same tests. They all led to the same result; only chi-square is shown in the paper.

The automatically measured orientation distributions were compared to each other with two-sample, two-sided Kolmogorov-Smirnov test. The two cell types that display each of the observed orientation patterns were compared using chi-square, likelihood ratio chi-square and Mantel-Haenszel chi-square tests. They yielded the same results.

Results

In this study, we analyzed chromosome 11 orientation patterns in lymphocytes of PCTs and of [T38HxBALB/c]N rcpT(X;11) mice. We performed mBANDing and analysis on more than 300 nuclei of each cell type. The mouse chromosome 11 mBAND probe labels four overlapping segments with four fluorescing colors. The telomeric end is labeled with FITC Green, the centromeric end with Texas Red, and

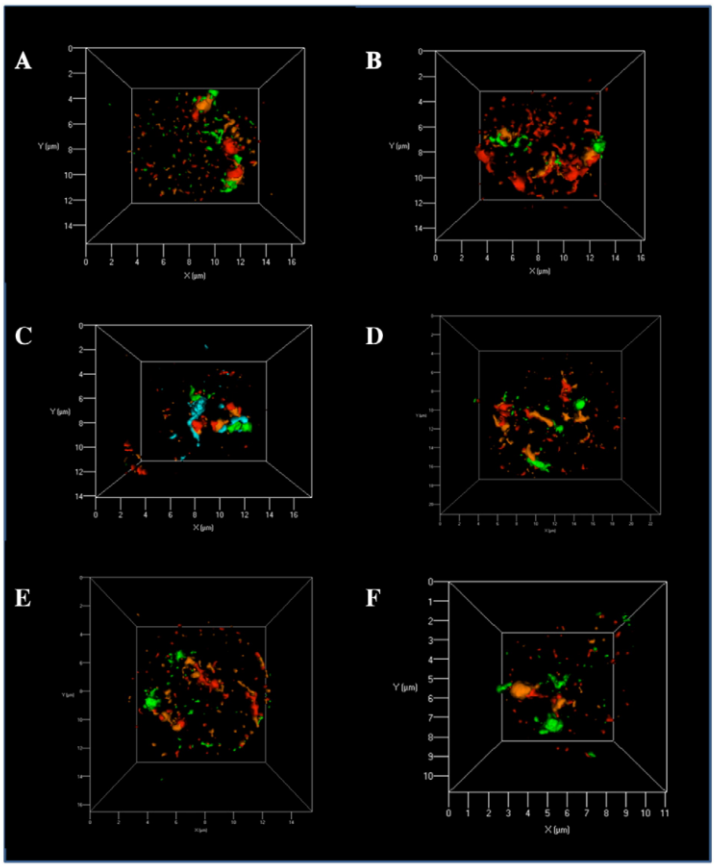

Figure 4. Representative 3D images of PCT and T38HT(X;11) nuclei with more than two copies of chromosome 11 and one image with T(X;11) present. The scale of the *x*- and *y*-axis is in [μ]. The telomeric end is labeled with FITC Green, the centromeric end with Texas Red, and the regions in between with Gold (orange) and DEAC (aqua blue). DEAC was not always detectable (C = centromere (magenta) points to periphery, T = telomere (green) points to periphery, P = chromosome is parallel to nuclear periphery). (A) PCT nucleus showing the orientation pattern "CPT." (B) PCT nucleus with the orientation pattern "CCT." (C) PCT nucleus with orientation pattern "CTT." (D) PCT nucleus with the orientation pattern "CCPP." (E) PCT nucleus showing the orientation pattern "TTT." (F) T38HT(X;11) nucleus with the orientation pattern "TT" and the small translocation chromosome T(X;11) in the center.

the regions in between with Gold and DEAC (Figure 2). The segment labeled with DEAC was not always detectable. The mBANDed nuclei were imaged using Axiovision 4.8 Software (Carl Zeiss Inc. Canada) and deconvolved with a constrained iterative algorithm [31]. By visual inspection, we analyzed the orientation of chromosome 11 of the respective cell types and subsequently determined orientation patterns. Nuclei of T38HT(X;11) lymphocytes consistently showed a diploid chromosome constitution, whereas nuclei of PCTs either were diploid or showed an increase in chromosome 11 copy numbers. Moreover, we identified the position of the small translocation chromosome T(X;11) in all nuclei of T38HT(X;11) and PCT.

By visual inspection, we observed three different orientations in nuclei of T38HT(X;11) and PCTs: 1) chromosome 11 points with its telomeric end to the nuclear periphery and with its centromeric end to the nuclear center ("T"); 2) it points with its centromeric end to the nuclear periphery and with its telomeric end to the center ("C"); and 3) chromosome 11 is in parallel to the nuclear border ("P"). Combining the observed orientations of all chromosomes in one nucleus, we determined an orientation pattern. All observed orientation patterns are shown in Table 1. The most frequently observed orientation pattern in T38HT(X;11) was with both chromosomes located in parallel to the nuclear border ("PP") (35.0%). In all PCTs, "PP" was only observed in 10.7% ($P < .01$). The orientation pattern "CP" with one homolog pointing with its centromeric end toward the nuclear periphery and the other homolog being in parallel was found most frequently in PCTs (13.4% of all PCTs) and in 23.7% of T38HT(X;11) ($P = .83$). Both chromosomes

Table 2. Nuclear Position of the Small Translocation Chromosome T(X;11) in Cells of Congenic [T38HxBALB/c]N Mice Showing T(X;11) and in Diploid, Triploid, and Tetraploid PCTs

Nuclear Position	T38H T[X;11]	All PCTs	Chi-Square
Periphery	14 (15.7%)	12 (17.1%)	.81
Intermediate	55 (61.8%)	52 (74.3%)	.10
Central	20 (22.5%)	6 (8.6%)	.02

The nuclear positions of T(X;11) were compared by chi-square analysis. There is no significant difference between the two cell types regarding the nuclear position of T(X;11) (P = .06). A chi-square value of P > .05 indicates that the frequency of the T(X;11) position is similar between the two cell types.

pointing with their centromeric ends toward the periphery ("CC") was observed in 18.7% of T38HT(X;11) and in 8.5% of all PCTs (P = .0001). The third most common orientation pattern in PCTs is "PT," with one homolog in parallel and the other pointing with its telomeric end to the periphery (8.5%). This orientation pattern was found in 13.6% of T38HT(X;11) (P < .01). Representative images of diploid PCT and T38HT(X;11) nuclei analyzed visually and automatically are illustrated in Figure 3.

Ninety-two of 224 (41.1%) PCT nuclei showed three copies of chromosome 11 (Table 1). The orientation pattern "CPT," with one copy pointing with its telomeric end and another copy with its centromeric end toward the nuclear periphery and one copy located in parallel, was also observed in 8.5% of all PCTs. The second most frequently orientation pattern in PCTs with three copies of chromosome 11 is "PPP," with all homologs located in parallel (7.6%).

Twenty-three of 224 (10.3%) PCT nuclei showed four copies of chromosome 11 (Table 1). Images of PCT nuclei with more than two copies of chromosome 11 can be seen in Figure 4.

When comparing T38HT(X;11) nuclei to all PCT nuclei with respect to their orientation patterns, a significant difference was noted (P < .0001). Regarding only diploid cells of PCTs and T38HT(X;11), there was no significant difference (P = .10). However, comparing diploid PCTs to PCTs with three or four copies of chromosome 11, a significant difference was noted (P < .0001).

For unknown reasons, the small translocation chromosome T(X;11) carrying cytoband 11E2 was only detected in 31.3% of all 224 mBANDed PCT nuclei and in 34.6% of the 257 mBANDed T38HT(X;11) nuclei. The most frequently observed position was in the intermediate region of the nucleus (61.8% of T38HT(X;11) and 74.3% of PCTs, respectively; P = .10) (Table 2). There is no significant difference between the two cell types regarding the position of T(X;11) (P = .0612). An image showing T(X;11) is demonstrated in Figure 4.

Discussion

We used mBANDing to determine the orientation of chromosome 11 in PCTs and lymphocytes of [T38HxBALB/c]N rcpT(X;11) mice, and we defined orientation patterns. In diploid nuclei of PCTs and T38HT(X;11), we found six distinct orientation patterns (Table 1). Most frequently observed was the orientation pattern "PP" (both chromosomes 11 in parallel to the nuclear border) in 35.0% of T38HT(X;11) and "CP" (one chromosome 11 is pointing with its centromeric end toward the nuclear periphery, whereas the other homolog is in parallel) in 13.4% of all PCTs. With respect to diploid nuclei of PCTs and diploid nuclei of T38H T[X;11] studied in this paper, we did not find a significant difference in the frequency of orientation patterns (P = .10). Analyzing PCT nuclei with three or four copies of chromosome 11, we found various orientation patterns (Table 1), e.g., the orientation pattern "CPT" (one homolog is pointing with its centromeric end and another with its telomeric end toward the nuclear center, and a third is in parallel) in 8.5% of all PCTs. When comparing PCT nuclei with three or four chromosome 11 copies to diploid PCT nuclei, a significant difference was noted (P < .0001). Furthermore, when comparing T38HT(X;11) to all PCT nuclei, we identified different orientation patterns (P < .0001).

The small translocation chromosome T(X;11) was analyzed visually and found in the intermediate region of the nucleus in 74.3% of the PCTs and in 61.8% of T38HT[X;11] (P = .10) (Table 2).

In our previous paper, we presented nonrandom orientation patterns for chromosome 11 in 3D nuclei of PreB lymphocytes of BALB/c origin and of [T38HxBALB/c]N wild-type mice [26]. There was a distinct difference between the frequency of the observed orientation patterns, and this was found in both cell types. The orientation pattern most frequently observed was with both chromosomes 11 in parallel to the nuclear periphery ("PP"). The second most common pattern was with one homolog in parallel and the other homolog pointed with its centromeric end toward the nuclear periphery ("CP").

The focus of the current study is the 3D nuclear orientation of chromosome 11 in mouse PCTs. We investigated changes in the nuclear orientation during the process of PCT development.

Nuclear architecture is important for nuclear function [5,9]. It is known that telomere dysfunction leads to genomic instability and therefore to tumorigenesis. Key factors of telomere dysfunction are the shortening of telomeres, breakage-bridge-fusion cycles, and the formation of telomeric aggregates (TAs) [32–34]. A trigger for TA formation is c-Myc deregulation [35]. Louis et al. (2005) described not only that c-Myc deregulation leads to TA formation resulting in breakage-bridge-fusion cycles but also that changes of nuclear positions lead to closer proximity of telomeres, resulting in chromosomal rearrangements [35]. Changes in chromosome orientation may also lead to closer proximity of telomeres and could therefore be linked to telomere aggregation.

Rotation is a way of movement and a possible way to change nuclear positions. The mechanisms of a possible rotation are currently unknown. One may hypothesize that chromosomes rotate to access transcription factories. The transcription of genes within the telomeric end 11E2 might be enhanced due to telomeric orientation toward the nuclear center. Future studies will elucidate these questions.

In conclusion, we found distinct 3D orientation patterns of mouse chromosome 11 in diploid lymphocytes of [T38HxBALB/c]N rcpT(X;11) mice and of PCTs. How and whether the changes of the orientation patterns in PCT nuclei with three or four chromosomes 11 impact on tumor progression will be the focus of future studies.

Acknowledgements

This study was supported by the Canadian Institutes of Health Research. A. K. S. received a travel award from Bayer. We thank Mary Cheang for statistical analysis. The authors declare that they have no competing interests.

References

[1] Tanabe H, Habermann FA, Solovei I, Cremer M, and Cremer T (2002). Non-random radial arrangements of interphase chromosome territories: evolutionary considerations and functional implications. *Mutat Res* **504**, 37–45.

[2] Cremer T and Cremer M (2010). Chromosome territories. *Cold Spring Harb Perspect Biol* **2**, a003889.

[3] Dyer KA, Canfield TK, and Gartler SM (1989). Molecular cytological differentiation of active from inactive X domains in interphase: implications for X chromosome inactivation. *Cytogenet Cell Genet* **50**, 116–120.

[4] Dietzel S, Schiebel K, Little G, Edelmann P, Rappold GA, Eils R, Cremer C, and Cremer T (1999). The 3D positioning of ANT2 and ANT3 genes within female X chromosome territories correlates with gene activity. *Exp Cell Res* **252**, 363–375.

[5] Solovei I, Kreysing M, Lanctot C, Kosem S, Peichl L, Cremer T, Guck J, and Joffe B (2009). Nuclear architecture of rod photoreceptor cells adapts to vision in mammalian evolution. *Cell* **137**, 356–368.

[6] Tam R, Smith KP, and Lawrence JB (2004). The 4q subtelomere harboring the FSHD locus is specifically anchored with peripheral heterochromatin unlike most human telomeres. *J Cell Biol* **167**, 269–279.

[7] Quina AS and Parreira L (2005). Telomere-surrounding regions are transcription-permissive 3D nuclear compartments in human cells. *Exp Cell Res* **307**, 52–64.

[8] Hanahan D and Weinberg RA (2011). Hallmarks of cancer: the next generation. *Cell* **144**, 646–674.

[9] Mai S (2010). Initiation of telomere-mediated chromosomal rearrangements in cancer. *J Cell Biochem* **109**, 1095–1102.

[10] De Vos WH, Hoebe RA, Joss GH, Haffmans W, Baatout S, Van Oostveldt P, and Manders EM (2009). Controlled light exposure microscopy reveals dynamic telomere microterritories throughout the cell cycle. *Cytometry A* **75**, 428–439.

[11] Molenaar C, Wiesmeijer K, Verwoerd NP, Khazen S, Eils R, Tanke HJ, and Dirks RW (2003). Visualizing telomere dynamics in living mammalian cells using PNA probes. *EMBO J* **22**, 6631–6641.

[12] Mehta IS, Amira M, Harvey AJ, and Bridger JM (2010). Rapid chromosome territory relocation by nuclear motor activity in response to serum removal in primary human fibroblasts. *Genome Biol* **11**, R5.

[13] Kuroda M, Tanabe H, Yoshida K, Oikawa K, Saito A, Kiyuna T, Mizusawa H, and Mukai K (2004). Alteration of chromosome positioning during adipocyte differentiation. *J Cell Sci* **117**, 5897–5903.

[14] Kim SH, McQueen PG, Lichtman MK, Shevach EM, Parada LA, and Misteli T (2004). Spatial genome organization during T-cell differentiation. *Cytogenet Genome Res* **105**, 292–301.

[15] Collins K and Mitchell JR (2002). Telomerase in the human organism. *Oncogene* **21**, 564–579.

[16] Greider CW and Blackburn EH (1985). Identification of a specific telomere terminal transferase activity in Tetrahymena extracts. *Cell* **43**, 405–413.

[17] Cesare AJ and Reddel RR (2010). Alternative lengthening of telomeres: models, mechanisms and implications. *Nat Rev Genet* **11**, 319–330.

[18] Kuzyk A and Mai S (2012). Selected telomere length changes and aberrant three-dimensional nuclear telomere organization during fast-onset mouse plasmacytomas. *Neoplasia* **14**, 344–351.

[19] Wiener F, Schmälter AK, Mowat MR, and Mai S (2010). Duplication of subcytoband 11E2 of chromosome 11 is regularly associated with accelerated tumor development in v-abl/myc–induced mouse plasmacytomas. *Genes Cancer* **1**, 847–858.

[20] Potter M and Wiener F (1992). Plasmacytomagenesis in mice: model of neoplastic development dependent upon chromosomal translocations. *Carcinogenesis* **13**, 1681–1697.

[21] Wiener F, Coleman A, Mock BA, and Potter M (1995). Nonrandom chromosomal change (trisomy 11) in murine plasmacytomas induced by an ABL-MYC retrovirus. *Cancer Res* **55**, 1181–1188.

[22] Koelsch BU, Rajewsky MF, and Kindler-Rohrborn A (2005). A 6-Mb contig-based comparative gene and linkage map of the rat schwannoma tumor suppressor region at 10q32.3. *Genomics* **85**, 322–329.

[23] Johansson B, Fioretos T, and Mitelman F (2002). Cytogenetic and molecular genetic evolution of chronic myeloid leukemia. *Acta Haematol* **107**, 76–94.

[24] Lastowska M, Chung YJ, Cheng Ching N, Haber M, Norris MD, Kees UR, Pearson AD, and Jackson MS (2004). Regions syntenic to human 17q are gained in mouse and rat neuroblastoma. *Genes Chromosomes Cancer* **40**, 158–163.

[25] Turhan N, Yurur-Kutlay N, Topcuoglu P, Sayki M, Yuksel M, Gurman G, and Tukun A (2006). Translocation (13;17)(q14;q25) as a novel chromosomal abnormality in acute myeloid leukemia-M4. *Leuk Res* **30**, 903–905.

[26] Schmälter AK, Kuzyk A, Righolt CH, Neusser M, Steinlein OK, Muller S, and Mai S (2014). Distinct nuclear orientation patterns for mouse chromosome 11 in normal B lymphocytes. *BMC Cell Biol* **15**, 22.

[27] Chudoba I, Plesch A, Lorch T, Lemke J, Claussen U, and Senger G (1999). High resolution multicolor-banding: a new technique for refined FISH analysis of human chromosomes. *Cytogenet Cell Genet* **84**, 156–160.

[28] Lemke J, Claussen J, Michel S, Chudoba I, Muhlig P, Westermann M, Sperling K, Rubtsov N, Grummt UW, and Ullmann P, et al (2002). The DNA-based structure of human chromosome 5 in interphase. *Am J Hum Genet* **71**, 1051–1059.

[29] Benedek K, Chudoba I, Klein G, Wiener F, and Mai S (2004). Rearrangements of the telomeric region of mouse chromosome 11 in Pre-B ABL/MYC cells revealed by mBANDing, spectral karyotyping, and fluorescence in-situ hybridization with a subtelomeric probe. *Chromosome Res* **12**, 777–785.

[30] Righolt CH, Schmälter AK, Kuzyk A, Young I, van Vliet L, and Mai S (2015). Measuring murine chromosome orientation in interphase nuclei. *Cytometry A* **87**(8), 733–740. http://dx.doi.org/10.1002/cyto.a.22674 [Epub 2015 Apr 17].

[31] Schaefer LH, Schuster D, and Herz H (2001). Generalized approach for accelerated maximum likelihood based image restoration applied to three-dimensional fluorescence microscopy. *J Microsc* **204**, 99–107.

[32] Chuang TC, Moshir S, Garini Y, Chuang AY, Young IT, Vermolen B, van den Doel R, Mougey V, Perrin M, and Braun M, et al (2004). The three-dimensional organization of telomeres in the nucleus of mammalian cells. *BMC Biol* **2**, 12.

[33] Mai S and Garini Y (2005). Oncogenic remodeling of the three-dimensional organization of the interphase nucleus: c-Myc induces telomeric aggregates whose formation precedes chromosomal rearrangements. *Cell Cycle* **4**, 1327–1331.

[34] Mai S and Garini Y (2006). The significance of telomeric aggregates in the interphase nuclei of tumor cells. *J Cell Biochem* **97**, 904–915.

[35] Louis SF, Vermolen BJ, Garini Y, Young IT, Guffei A, Lichtensztejn Z, Kuttler F, Chuang TC, Moshir S, and Mougey V, et al (2005). c-Myc induces chromosomal rearrangements through telomere and chromosome remodeling in the interphase nucleus. *Proc Natl Acad Sci U S A* **102**, 9613–9618.

8 References

Benedek, K., I. Chudoba, G. Klein, F. Wiener, and S. Mai. 2004. 'Rearrangements of the telomeric region of mouse chromosome 11 in Pre-B ABL/MYC cells revealed by mBANDing, spectral karyotyping, and fluorescence in-situ hybridization with a subtelomeric probe', *Chromosome Res*, 12: 777-85.

Bird, A. 2007. 'Perceptions of epigenetics', *Nature*, 447: 396-8.

Chan, S. R., and E. H. Blackburn. 2004. 'Telomeres and telomerase', *Philos Trans R Soc Lond B Biol Sci*, 359: 109-21.

Chudoba, I., A. Plesch, T. Lorch, J. Lemke, U. Claussen, and G. Senger. 1999. 'High resolution multicolor-banding: a new technique for refined FISH analysis of human chromosomes', *Cytogenet Cell Genet*, 84: 156-60.

Cremer, T., and M. Cremer. 2010. 'Chromosome territories', *Cold Spring Harb Perspect Biol*, 2: a003889.

Dyer, K. A., T. K. Canfield, and S. M. Gartler. 1989. 'Molecular cytological differentiation of active from inactive X domains in interphase: implications for X chromosome inactivation', *Cytogenet Cell Genet*, 50: 116-20.

Hepperger, C., A. Mannes, J. Merz, J. Peters, and S. Dietzel. 2008. 'Three-dimensional positioning of genes in mouse cell nuclei', *Chromosoma*, 117: 535-51.

Heride, C., M. Ricoul, K. Kieu, J. von Hase, V. Guillemot, C. Cremer, K. Dubrana, and L. Sabatier. 2010. 'Distance between homologous chromosomes results from chromosome positioning constraints', *J Cell Sci*, 123: 4063-75.

Kalitsis, P., B. Griffiths, and K. H. Choo. 2006. 'Mouse telocentric sequences reveal a high rate of homogenization and possible role in Robertsonian translocation', *Proc Natl Acad Sci U S A*, 103: 8786-91.

Koelsch, B. U., M. F. Rajewsky, and A. Kindler-Rohrborn. 2005. 'A 6-Mb contig-based comparative gene and linkage map of the rat schwannoma tumor suppressor region at 10q32.3', *Genomics*, 85: 322-9.

Kouzarides, T. 2007. 'Chromatin modifications and their function', *Cell*, 128: 693-705.

Kupper, K., A. Kolbl, D. Biener, S. Dittrich, J. von Hase, T. Thormeyer, H. Fiegler, N. P. Carter, M. R. Speicher, T. Cremer, and M. Cremer. 2007. 'Radial chromatin positioning is shaped by local gene density, not by gene expression', *Chromosoma*, 116: 285-306.

Kuzyk, A., S. Booth, C. Righolt, S. Mathur, J. Gartner, and S. Mai. 2015. 'MYCN overexpression is associated with unbalanced copy number gain, altered nuclear location, and overexpression of chromosome arm 17q genes in neuroblastoma tumors and cell lines', *Genes Chromosomes Cancer*, 54: 616-28.

Kuzyk, A., and S. Mai. 2012. 'Selected telomere length changes and aberrant three-dimensional nuclear telomere organization during fast-onset mouse plasmacytomas', *Neoplasia*, 14: 344-51.

Lanctot, C., T. Cheutin, M. Cremer, G. Cavalli, and T. Cremer. 2007. 'Dynamic genome architecture in the nuclear space: regulation of gene expression in three dimensions', *Nat Rev Genet*, 8: 104-15.

Langan, J. E., C. G. Cole, E. J. Huckle, S. Byrne, F. E. McRonald, L. Rowbottom, A. Ellis, J. M. Shaw, I. M. Leigh, D. P. Kelsell, I. Dunham, J. K. Field, and J. M. Risk. 2004. 'Novel microsatellite markers and single nucleotide polymorphisms refine the tylosis with oesophageal cancer (TOC) minimal region on 17q25 to 42.5 kb: sequencing does not identify the causative gene', *Hum Genet*, 114: 534-40.

Mai, S., and Y. Garini. 2005. 'Oncogenic remodeling of the three-dimensional organization of the interphase nucleus: c-Myc induces telomeric aggregates whose formation precedes chromosomal rearrangements', *Cell Cycle*, 4: 1327-31.

Mai, S., and Y. Garini. 2006. 'The significance of telomeric aggregates in the interphase nuclei of tumor cells', *J Cell Biochem*, 97: 904-15.

Marella, N. V., B. Seifert, P. Nagarajan, S. Sinha, and R. Berezney. 2009. 'Chromosomal rearrangements during human epidermal keratinocyte differentiation', *J Cell Physiol*, 221: 139-46.

Mehta, I. S., M. Amira, A. J. Harvey, and J. M. Bridger. 2010. 'Rapid chromosome territory relocation by nuclear motor activity in response to serum removal in primary human fibroblasts', *Genome Biol*, 11: R5.

Morey, C., C. Kress, and W. A. Bickmore. 2009. 'Lack of bystander activation shows that localization exterior to chromosome territories is not sufficient to up-regulate gene expression', *Genome Res*, 19: 1184-94.

Righolt, C. H., A. K. Schmalter, A. Kuzyk, I. T. Young, L. J. van Vliet, and S. Mai. 2015. 'Measuring murine chromosome orientation in interphase nuclei', *Cytometry A*, 87: 733-40.

Russo, V. E. A., Robert A. Martienssen, and Arthur D. Riggs. 1996. *Epigenetic mechanisms of gene regulation* (Cold Spring Harbor Laboratory Press: Plainview, N.Y.).

Schaefer, L. H., D. Schuster, and H. Herz. 2001. 'Generalized approach for accelerated maximum likelihood based image restoration applied to three-dimensional fluorescence microscopy', *J Microsc*, 204: 99-107.

Solovei, I., A. Cavallo, L. Schermelleh, F. Jaunin, C. Scasselati, D. Cmarko, C. Cremer, S. Fakan, and T. Cremer. 2002. 'Spatial preservation of nuclear chromatin architecture during three-dimensional fluorescence in situ hybridization (3D-FISH)', *Exp Cell Res*, 276: 10-23.

Solovei, I., M. Kreysing, C. Lanctot, S. Kosem, L. Peichl, T. Cremer, J. Guck, and B. Joffe. 2009. 'Nuclear architecture of rod photoreceptor cells adapts to vision in mammalian evolution', *Cell*, 137: 356-68.

Turhan, N., N. Yurur-Kutlay, P. Topcuoglu, M. Sayki, M. Yuksel, G. Gurman, and A. Tukun. 2006. 'Translocation (13;17)(q14;q25) as a novel chromosomal abnormality in acute myeloid leukemia-M4', *Leuk Res*, 30: 903-5.

Volpi, E. V., E. Chevret, T. Jones, R. Vatcheva, J. Williamson, S. Beck, R. D. Campbell, M. Goldsworthy, S. H. Powis, J. Ragoussis, J. Trowsdale, and D. Sheer. 2000. 'Large-scale chromatin organization of the major histocompatibility complex and other regions of human chromosome 6 and its response to interferon in interphase nuclei', *J Cell Sci*, 113 (Pt 9): 1565-76.

Wiener, F., A. K. Schmalter, M. R. Mowat, and S. Mai. 2010. 'Duplication of Subcytoband 11E2 of Chromosome 11 Is Regularly Associated with

Accelerated Tumor Development in v-abl/myc-Induced Mouse Plasmacytomas', *Genes Cancer*, 1: 847-58.

Acknowledgements

I thank Prof. Dr. med. Ortrud Steinlein who made the cooperation between the Institute of Human Genetics of the Ludwig-Maximilians-University Munich, Germany and the Manitoba Institute of Cell Biology, Manitoba University, Winnipeg, Canada possible.

Special thanks goes to Prof. Sabine Mai for giving me the chance to be part of her research team, designing the study and making both publications a success. With her great support throughout all the years and her confidence in me and my work she became a mentor and a friend to me.

I sincerely thank PD Dr. rer. nat. Stefan Müller for his competent and motivating support and his helpful advice.

I also thank Dr. Christiaan Righolt, Dr. rer. nat. Michaela Neusser and Alexandra Kuzyk for their help with the publications.

Many thanks to my family and friends for their support in every way.

Eidesstattliche Versicherung

Schmälter, Ann-Kristin

Name, Vorname

Ich erkläre hiermit an Eides statt,

dass ich die vorliegende Dissertation mit dem Thema

Nuclear orientation patterns for mouse chromosome 11 in normal B lymphocytes and during plasmacytoma development

selbständig verfasst, mich außer der angegebenen keiner weiteren Hilfsmittel bedient und alle Erkenntnisse, die aus dem Schrifttum ganz oder annähernd übernommen sind, als solche kenntlich gemacht und nach ihrer Herkunft unter Bezeichnung der Fundstelle einzeln nachgewiesen habe.

Ich erkläre des Weiteren, dass die hier vorgelegte Dissertation nicht in gleicher oder in ähnlicher Form bei einer anderen Stelle zur Erlangung eines akademischen Grades eingereicht wurde.

Ort, Datum

Unterschrift Doktorandin/Doktorand